

Appendix VII
Manuscript

Title: Changes in epidermal and sub-epidermal structures related to the molting cycle of the black tiger shrimp, *Penaeus monodon*.

Authors: Waraporn Promwikorn^{1*}, Pornpimol Kirirat¹, Pranom Intasaro¹ and Boonsirm Withyachumnarnkul².

Address: ¹ Department of Anatomy, Faculty of Science, Prince of Songkla University, Hat-Yai, Songkhla, Thailand, 90112. ² Department of Anatomy and Center of Excellence for Shrimp Molecular Biology and Biotechnology, Faculty of Science, Mahidol University, Bangkok, Thailand, 10400.

***Correspondence:** Dr. Waraporn Promwikorn, Department of Anatomy, Faculty of Science, Prince of Songkla University, Hat-Yai, Songkhla, Thailand, 90112, Tel. +66 74288135, Fax. +66 74446663, E-mail: waraporn.p@psu.ac.th

Number of text pages: 30 pages

Number of figures: 14 figures

Abbreviated title: Epidermal changes during shrimp's molting cycle

Keywords: epidermis, sub-epidermis, molting cycle, *Penaeus monodon*

Abstract

Previous studies of crabs and lobsters have established that the integument plays an important role in the shedding and replacement of their cuticle. In this study we have investigated the morphological and ultra-structural changes that occur in the epidermis and sub-epidermis of the black tiger shrimp (*Penaeus monodon*), an important agricultural export product of Thailand, during its molting cycle, using histochemical and electron microscopy techniques. We investigate cell morphology and ultra-structures of the epidermis and sub-epidermis related to the molting cycle by histochemical and electron microscopic techniques. The epidermis consists of a single cell layer located beneath the cuticle, and changes occur in cell height during the molting cycle. The cell height is greatest during the mid premolt to early postmolt period when the cells are metabolically most active. The epidermis is composed of two cell types, a major, type I type and a minor, type II type. They have different characteristics and ultra-structures, indicating that they play different roles. The type I epidermal cell is most likely responsible for the synthesis of protein and micro-fibers, whereas the type II cell is most likely involved in the synthesis of protein and carbohydrate required for the new cuticle. The sub-epidermis is mainly composed of sub-epidermal cells and tegumental glands. We found that the sub-epidermis serves as a store of carbohydrate, protein, mucus and other unidentified substances. The storage of carbohydrate and protein is greatest at the time when the epidermal cells are tallest. The results confirm that in the black tiger shrimp the epidermis and sub-epidermis are responsible for cuticular regeneration, and the period of greatest activity is during the mid premolt to early postmolt stages. For the first time, this work provides direct evidence of the epidermal and sub-epidermal changes that occur during the molting cycle of the black tiger shrimp.

Introduction

In crustaceans, the cycle of post-embryonic growth and development is characterized by a unique molting cycle. Each molting cycle has various stages including pre-ecdysis (premolt, D0-4 stages), ecdysis (E stage), post-ecdysis (postmolt, A1-2, B1-2 and C1-2 stages), and intermolt (C3-4 stages) stages (Drach, 1939; Skinner, 1962). The progression of each molting cycle is regulated by the balance of the molt-stimulating ecdysteroid hormones, which are secreted by pairs of Y-organs and mandibular organs located at the oral region (Carlisle, 1957; Hubschman and Armstrong, 1972; Aoto *et al.*, 1974; Byard *et al.*, 1975; Hinsch and Hajj, 1975; Keller and Willig, 1976; Keller and Schmid, 1979; Yudin *et al.*, 1980; Watson and Spaziani, 1985; Homola and Chang 1997; Spaziani *et al.*, 1999; Borst *et al.*, 2001; Chang, 2001; Nagaraju *et al.*, 2004), and molt-inhibiting hormone, which is secreted from the X-organ sinus gland complex located in the eyestalk (Hubschman and Armstrong, 1972; Rao, 1973; Freeman and Costlow, 1979; Gersch, 1979; Soumoff and O'Connor, 1982; Nakatsuji and Sonobe, 2004). In conjunction with the molting cycle, there are dramatic changes in body and organ structures (Skinner, 1962; Miyawaki and Taketomi, 1984; Taketomi and Hyodo, 1986; Rahman and Subramoniam, 1989; Sousa and Petriella, 2001; Pratoomchat *et al.*, 2002b; Nagaraju *et al.*, 2004), physiology and biochemistry (Glynn, 1968; Burse and Lane, 1971; Hubschman and Armstrong, 1972; Teshima *et al.*, 1975; Brannon and Rao, 1979; Huner *et al.*, 1979a, b; Favrel, *et al.*, 1987; Graf and Delbecque, 1987; Bellon-Humbert and Van Herp, 1988; Walgraeve *et al.*, 1988; Cuzin-Roudy *et al.*, 1989; Mercaldo-Allen, 1991; Spindler *et al.*, 1992; Scott-Fordsmand and Depledge, 1997; Meunpol *et al.*, 1998; Terwilliger *et al.*, 1999; Fernandez-Gimenez *et al.*, 2001; Sousa and Petriella, 2001; Aragon *et al.*, 2002; Fernandez-Gimenez *et al.*, 2002; Pratoomchat *et al.*, 2002a; Wang *et al.*, 2003; Gunamalai *et al.*, 2004; Nakatsuji and Sonobe, 2004) and behavior (Morgan, 1978; Tamm and Cobb, 1978; Lipcius and Herrnkind, 1982). The main purpose of the molting process is to shed the cuticle off the animal's body to allow for an increase in body mass before the newly synthesized cuticle becomes fully calcified during the postmolt period. During the premolt stages the cuticle is gradually degraded by the re-absorption of organic and inorganic materials, deposited in the cuticle, back to the shrimp's body for reuse after ecdysis, concurrently with the synthesis of the pre-ecdysial layer. After ecdysis, the new cuticle replaces the old one, concurrently with the secretion of organic and inorganic materials from the shrimp's body back to the cuticle for the synthesis of post-ecdysial layer. The main organs and tissues, responsible for this crucial task, include the epidermis, haemolymph, hepatopancreas and

stomach. The epidermis (sometimes referred as “hypodermis”) is located underneath the cuticle, and is a target for ecdysteroids (Traub *et al.*, 1987; Ueno *et al.*, 1992). The epidermis is directly involved in the re-absorption and secretion of organic and inorganic materials from and to the cuticle (Roer and Dillaman, 1984; Machado *et al.*, 1990; Compere *et al.*, 1993; Ziegler, 1996; Hagedorn and Ziegler, 2002; Pratoomchat *et al.*, 2002a). During these tasks, the cellular activities of the epidermal cells change dramatically depending on the stage of the molting cycle.

It is reported that the epidermal DNA content of the western rock lobster *Panulirus longipes* increases during early premolt and thereafter declines, while the RNA content steadily increases from stage D1 and almost doubles by stage D4 of the premolt period (Wittig and Stevenson, 1975; Dall and Barclay, 1979). The rate of protein synthesis in the epidermis of crab and crayfishes is highest at the D2 stage, and declines afterwards (Skinner, 1966; McWhinnie and Mohrherr, 1970; Humphreys and Stevenson, 1973). Proteins in the cuticle-epidermis of the white shrimp *Penaeus vannamei* (Cariolou and Flytzanis, 1994), and the crayfish *Astacus leptodactylus*-I (Bielefeld *et al.*, 1986) are differentially expressed during the molting cycle. Some of the genes and proteins of the epidermis involved in this mechanism have been identified and named. These include the cryptocyanin protein in crab *Cancer magister* (Terwilliger and Otsoshi, 1994), chitinase gene (Pjchi-2) in the Kuruma prawn *Penaeus japonicus* (Watanabe and Kono, 1997), DD4, DD5, DD9A and DD9B genes in the prawn *Penaeus japonicus* (Endo *et al.*, 2000; Watanabe *et al.*, 2000; Ikeya *et al.*, 2001), and prophenoloxidase-activating factor of the blue crab, *Callinectes sapidus* (Buda and Shafer, 2005). Changes of epidermal and sub-epidermal histology that occur during the molting cycle have been reported in various species of crabs and lobsters (Travis, 1955; Skinner, 1962; Stevenson *et al.*, 1968; Green and Neff, 1972; Schultz and Kennedy, 1977). It is reported that the size of epidermal cells increase during premolt, and diminish during postmolt stages (Travis, 1955; Skinner, 1962; Green and Neff, 1972; Schultz and Kennedy, 1977), while the sub-epidermal tissue stores lipoprotein for the developing cuticle (Travis, 1955; Skinner, 1962; Green and Neff, 1972). Overall findings, from both the histological and molecular levels, have led to a better understanding of the regulatory mechanisms involved in molting. However this knowledge has been obtained using various crustacean species, and the finer details of any one mechanism are still unknown.

We have been gathering information on the regulatory mechanisms of the molting cycle in the black tiger shrimp (*Penaeus monodon*), which is an important agricultural export product of Thailand. We recently reported on the criteria used for determining the molting stages of this particular species (Promwikorn *et al.*, 2004) and on the histological characterization of collagen fibers, carbohydrate, protein, lipid, and calcium salt deposited in the cuticle throughout the molting cycle (Promwikorn *et al.*, 2005). In this study we aim to investigate changes in cell morphology and ultra-structure of the epidermis and sub-epidermis occurring during the molting cycle in order to achieve a better understanding of the molting mechanisms of this species. For the first time, this work will provide direct evidence of the epidermal and sub-epidermal changes that occur during the molting cycle of *Penaeus monodon*.

Materials and methods.

Animals

Healthy black tiger shrimps (*P. monodon*) were obtained from commercial farms. During transportation to our laboratory in PSU, the shrimps were continuously oxygenated. The age of the shrimps was estimated at about 90 days, and their body weights were between 10-20 g.

Shrimp culture

Natural sea water, used in all experiments, was stored in a tank for at least 2 weeks before use. Some days before the experiments, the sea water in the aquarium was continuously aerated. The salinity was adjusted to be similar to the sea water used in the farms (10-30 ppt. depending on the salinity of each farm). Once the shrimps had arrived, the molting stage of each shrimp was determined prior to its cultivation with continuous aeration. The shrimps were fed three times a day with commercial pellet. Natural day-light and atmospheric temperatures (28-34 °C) were used throughout the experiment.

Determination of molting stages

Daily physical examinations were made to determine the molting stages. Briefly, each shrimp was gently picked by hand. The uropods locating at the level of the tip of the telson were then quickly examined with a light microscope. The physical criteria used for determining the molting stage are described in the results section. After 1–2 min examination, the shrimps

were either placed back into the aquarium, or executed. For every shrimp, the molting stages were next confirmed by histological criteria.

Histological study

The cuticular tissues at the carapace and trunk (first abdominal somite) of at least 10 shrimps at each molting stage were dissected and immediately fixed in Davidson's fixative to eliminate any calcium salt in the cuticle. The fixation stage was continued for 72 h at room temperature with a daily change of fresh fixative. The cuticular tissues were subsequently dehydrated in increasing concentrations of ethanol that ranged from 50 to 100%, and prepared for routine histological embedding in paraffin blocks. Paraffin sections (0.5 μm thick) were routinely de-paraffinized and stained for collagen fibers with modified Masson's trichrome (aniline blue, ponceau S, hematoxylin) (Bancroft and Gamble modification, 2002a), and carbohydrate (with periodic acid Schiff's reagent, PAS) (Bancroft and Gamble, 2002b). The stained tissue sections were examined with a light microscope (Olympus BX 51) and photographed with a digital camera (Olympus DP11) connected to the microscope.

Transmission electron microscopic study

The cuticular tissues at the carapace of 2-3 shrimps at each molting stage were cut into pieces, with an approximate size of 0.1 x 0.1 mm, and immediately immersed in TEM fixative (4% paraformaldehyde, 2.5% glutaraldehyde in 0.1 M PBS pH 7.2 ($\text{NaH}_2\text{PO}_4 \cdot \text{H}_2\text{O}$, Na_2HPO_4) for 48 h at 4 °C. The tissues were then washed twice with 0.1 M PBS pH 7.2 to remove the fixative before either continuing with further procedures, or storing in the same solution until used. All further procedures were carried out at room temperature. The tissues were washed once with the phosphate buffer solution, and immersed in 1% OsO_4 in 0.1 M PBS pH 7.2 for 1 h. The tissues were next washed twice with distilled water, then immersed in 2% uranyl acetate in 70% methanol for 20 min, and dehydrated through a series of increasing ethanol concentrations ranging from 70 to 100%. The tissues were then infiltrated with propylene oxide for 15 min and the process repeated. This was replaced with a 1:1 ratio of propylene oxide and epoxy resin for 1 h, followed by a 1:2 ratio of propylene oxide and epoxy resin for 1 h before embedding in epoxy resin, and leaving for polymerisation at 70 – 80 °C for 12 – 24 h. Sections of the samples of 60 – 90 nm thickness were obtained with an ultra-microtome (MTXL, RMC), and stained with lead acetate-sodium citrate mixture and 5% uranyl acetate in 70% methanol before being photographed with an electron microscope (Jeol JEM-100 CX II).

The negatives were exposed on Kodak photographic papers and developed with Kodak materials.

Results

1. Determination of the molting stages.

Identification of the molting stage is based primarily on the physical characteristics of the cuticular tissue. In the intermolt stage, the setal cones (SCs) of shrimps are fully developed and arranged in a neat line at the base of the setae. The epidermal tissue, which is located interior to the cuticle, is spreading throughout the area under the cuticle and between pairs of SCs (C stage, Fig. 1a). Once the epidermal tissue begins to retract away from the cuticle the shrimp is designated as being at stage D0. An observed clear straight margin of the epidermal tissue at the base of the SCs determines the ending of the D0 stage (Fig. 1b). The D1 stage is defined by the appearance of a narrow clear zone between the SCs and the epidermal tissue (Fig. 1c). The clear zone is the site for the formation of a new cuticle. In the D2 stage, the width of the clear zone between the SCs and the epidermal tissue increases, and the edge of the epidermal tissue now has a wave-like pattern. Small and thin fiber-like projections between SCs and epidermal tissue are also observed (Fig. 1d). These projections would later become new setae. The D3 stage is designated, when the clear zone between the SCs and the epidermal tissue has clearly widened, a thin white layer at the edge of the epidermal tissue appears together with a sharp-wavy edge of the epidermal tissue, and the fiber-like projections are easier to see (Fig. 1e). At the last stage of the premolt, the D4 stage, the synthesis of new cuticle continues until the clear zone between the SCs and epidermal tissue is extremely clear and dominant. The typical characteristics of the epidermal tissue are now clearly marked. As the white layer at its edge is reflecting the light, and forms sharp and serrate notches, young setae are clearly seen projecting from the impressions between the sharp notches. The pigments in the epidermal tissue are obviously indented and arranged in a paralleled-band fashion. The SCs then start to deform (Fig. 1f). Once the D4 stage is identified, the shrimp will be shedding the exuviae (the old cuticle, Fig. 2) within 24 hours. After examination, we found that the exuviae is composed of two pieces. The major piece is composed of most of the shrimp cuticle including the ventral part of the head, the trunk, the tail and all appendages. The minor piece is composed of carapace and rostrum. After ecdysis the shrimps immediately enter the postmolt A stage, in which the new cuticle and the setae are very soft

and delicate. The SC is not yet seen (Fig. 1g). Only a few hours after ecdysis, the shrimps enter postmolt B stage where the cuticle is hardening, and young SCs are developing. Different sizes of SCs are thus observed at the base of the setae (Fig. 1h). When the development of the SCs is completed, the shrimps enter C stage (Fig. 1a). The average timing of the molting cycle is 9-12 days with the premolt stages lasting for 6-7 days, the postmolt stages for 2-3 days, and intermolt stages for 1-2 days (Fig. 3).

After the molting stages are identified by their physical characteristics, the cuticle of the shrimps from each molting stage is subjected to a histological examination. After Periodic Acid Schiff's (PAS) staining, the mature cuticle of the shrimp intermolt stage (C3-4 stage) is observed to have four distinctive layers based on the texture and characteristics of the tissue (Fig. 4a). The most outer layer, an epicuticle, is thin and stains a deep magenta. The rest of the cuticle is a procuticle, which can be divided into three distinctive sub-layers from the exterior to interior; an exocuticle, an endocuticle and a membranous layer. The exocuticle, which lies next to the epicuticle, stains dark blue and consists of a series of alternating light and indented lamellae. The endocuticle, which lies next to the exocuticle, is characterised by a fine lamellae characteristic, and stains with PAS giving a more pink colour than the exocuticle. Lastly, the membranous layer, which lies between the endocuticle and epidermis, has a similar texture to the endocuticle, and can be distinguished by a darker staining reaction (Fig. 4a). It is noted that after staining with Masson's trichrome, the epicuticle stains red, while the procuticle stains blue (Fig. 5). During the early premolt period (D0-2), the epicuticle and exocuticle are still well-recognised, but the endocuticle and a membranous layer are stained light pink with PAS (Fig. 4b-c). The D3 stage begins, when a newly secreted epicuticle is just seen at the inner border of the old cuticle (Fig. 4d). In the D4 stage, the newly secreted exocuticle is observed between the new epicuticle and the underlying epidermis (Fig. 4e). Immediately after ecdysis, during the A1 - 2 stages, an epicuticle, and an exocuticle are observed in the intact cuticle (Fig. 4f). Ten hours after ecdysis when the shrimps are in the B1 stage, a small pink layer of newly secreted endocuticle is just seen at the inner border of the exocuticle (Fig. 4g). Two days after ecdysis, the thickness of the newly synthesized endocuticle increases (Fig. 4h). The shrimps are now in the B2 stage.

2. Morphology of the epidermis related to the molting cycle.

Histological methods were used to study the epidermal morphology of the trunk and carapace of the shrimp during various molting stages. In general the epidermis is composed of cells organized into a single row beneath the cuticle. The organization and height of the epidermal cells change throughout the molting cycle. The gap, that in some pictures appear between the cuticle and epidermal cells, is caused by the sliding of the cuticle away from the epidermis during histological procedures (Fig. 5).

During the intermolt stage the morphology of the row of epidermal cells, although not tidily organize, had an average height of 3.12 μm (Fig. 5a). During the development of the premolt period, the cell height gradually increases. Thus the shape of the cell changes into that of a tall column (Fig. 5b-e). The average cell height during the D2-4 stages (mid-late premolt stages) is 8.75 μm , which is an approximately 2.8 times increase from that of the intermolt stage and their arrangement becomes much tidier. After exoskeleton shedding, the epidermal cell height gradually decreases (Fig. 5f-h). The average cell height at the B1-2 stages is 7.33 μm .

Two types of the cells are distinguished by Masson's trichrome and PAS staining (Figs. 5, 6). The majority of the epidermal cells locate side-by-side, and the minority are scattered among the majority cells. The majority cells stain dark blue with trichrome and PAS. The minority stain only palely with Masson's trichrome, but deep pink with PAS. The latter cells have long apical cytoplasmic extensions, which traverse the canal that forms across the cuticle (Fig. 6a, b). The extensions reach to the epicuticle, which is the most outer layer of the cuticle (Fig. 6c). The number of these cells increases during the early premolt to early postmolt stages, decreases after the mid-postmolt stage, and are very hard to identify during the intermolt stage (Fig. 5).

3. Ultra-structures of the epidermis throughout the molting cycle.

Transmission electron microscopy was used to investigate the ultra-structures of the epidermal cells. We found that, in general, the epidermal cells were located in one row between the collagen fiber bundles and fibroblasts at the basal side, and the cuticle, which is at the apical side of the cells. Two types of epidermal cells are seen in the same row (Fig. 7). One type is the major type of epidermal cell, and the second type, located at random between

the major types, is rarely found. The ultra-structures of the major type of epidermal cell change during the molting cycle.

During the early premolt period (D2 stage), the major type cells have a tall columnar shape, and are tidily organized side by side to each others. Each cell possesses an elongated euchromatic nucleus (Fig. 7), numerous rough endoplasmic reticulum (RER), micro-fibers, free ribosomes, mitochondria, electron-dense vesicles and granules, which are distributed throughout the cytoplasm (Fig. 7). Interestingly, the micro-fibers are organized into compact bundles, and longitudinally arranged from the base to top of the cells (Fig. 8). At the top of the cells, the micro-fiber bundles become more electron-dense, and are attached to the cuticle. At several points, they pierce into, and become part of the cuticle (Fig. 8a).

During the late premolt period (D3-4 stage), the epidermal cell still has a tall columnar shape with an elongated euchromatic nucleus. The content of the cytoplasm is denser than that at the D2 stage, because of the increase in the amount of RER, free ribosomes, and granules (Fig. 8c). The spaces widen between epidermal-epidermal cells (intercellular space) and epidermal cells-connective tissue underneath (basal space), and groups of round electron-dense granules appear (Fig. 9a, b). Similar granules are also found beneath the epidermal layer near to the haemolymphatic sinus located nearby (Fig. 9b, d).

The plasma membrane at the intercellular and basal spaces develops cytoplasmic protusions, thus making a rough margin and producing tortuous intercellular and basal spaces (Figs. 9a, b, 12c). Many mitochondria are observed near these spaces. The apex of the cell is still firmly attached to the cuticle. The phenomenon of micro-fibers traversing the apical cytoplasm and piercing the cuticle is commonly observed, while the thickness of the newly synthesized cuticle is increasing (Fig. 8c). Numerous small electron-dense secretory vesicles are located at the top of the cells close to the cuticle (Fig. 8c). Just before ecdysis, the micro-fibers from the apical cytoplasm, that pierce the cuticle, now terminate just under the cuticle (Fig. 9c). Small electron-dense secretory vesicles, which are located at the top of the cells close to the cuticle, are still observed, but in smaller numbers.

During the early postmolt stages (A stage), the epidermal cell is still tall, but has a round nucleus. The cytoplasm contains numerous free ribosomes and electron-translucent vesicles,

especially at the apex of the cell (Fig. 10b). Electron-dense vesicles and granules are less commonly observed. In contrast to the premolt stage, the apex of the cell forms long cytoplasmic extensions, which traverse into the apical space between the epidermal cells and the cuticle, where numerous secretory vesicles and electron-dense precipitations are concentrated (Fig. 10a). It is noted that the newly secreted cuticle, which lies over the epidermal cells, contains moderately dense oval shaped-vesicles hence giving the unique characteristics of the cuticle for the postmolt stage. These vesicles have similar characteristics to the vesicles found in the apical space, and in the cytoplasm of the epidermal cells (Fig. 10a). Figure 10a shows small connecting paths between the apical space and newly synthesized cuticle (arrows).

During the mid-late postmolt stages (B stage), the cell and its nucleus develop an irregular shape (Fig. 11a). The intercellular and apical spaces become narrower than those found in the late premolt (D4) stage, however, they are still easily recognized. Numerous long cytoplasmic extensions are observed in the intercellular and apical spaces (Fig. 11b). Large electron-translucent secretory vesicles are located in the cell near these spaces, concurrently with mitochondria lying around the vesicles (Fig. 11a, c).

When the shrimp enters the intermolt stage, the epidermal cells become small, irregular shaped, and untidy (Fig. 12b). The tortuous intercellular spaces are still clearly observed, however, the apical space is not seen (Fig. 12a). Instead of cytoplasmic extensions, the apex of the cell is closely attached to the cuticle by developing electron-dense attachments to form a slim electron-dense band parallel to the cuticle (Fig. 12b). The micro-fibers still form the major content of the cytoplasm. Considerable amounts of RER and mitochondria are found throughout the cytoplasm, and particularly near the intercellular space. All secretory vesicles and granules are diminished.

We did not investigate the minority cell type related to the molting stage, as we could not find this cell type in every sample. However, we did find that at the early premolt stage (D2 stage) they have distinctive characteristics, but have a similar shape to the majority cell type. They develop cytoplasmic processes at the apical part of the cell (Figs. 7, 13a). The cytoplasm is denser, and richer in electron-dense vesicles, but there is less endoplasmic reticulum observed than in any of the other types (Fig. 13b).

4. Histology of sub-epidermal tissue related to the molting cycle.

The sub-epidermis is the tissue located just inside the epidermis, and can only be detected in some regions of the shrimp including the carapace and the free edge of the cuticle wrapping the trunk. PAS staining, shows that the sub-epidermal tissue is composed of mainly sub-epidermal (SE) cells, tegumental glands and some other connective tissue cells. The SE cells are oval shaped and sit very close together. Each cell has one centrally located nucleus. In some molting stages, the cytoplasm is stained pink after PAS (Fig. 14c-d), and stains red after modified Masson's trichrome staining with Ponceau S (Fig. 14f). However, in certain molting stages the cytoplasm of the SE cell is un-stained. Two types of tegumental glands are distributed among the SE cells throughout the sub-epidermis. A tegumental gland type A is strongly stained with PAS (Fig. 14b). After staining with toluidine blue dense granules are abundantly observed within the gland, except at the nuclear region (Fig. 14g). The boundaries of the cells are not clearly delineated. A tegumental gland type B is also positively stained with PAS, but less intensely. The contents of the cytoplasm are apparently mixed with mucus throughout the gland (Fig. 14c-d). When this gland is stained with toluidine blue, it gives a pink colour instead of blue (metachromasia reaction), but the area occupied by mucus is left un-stained (Fig. 14h). The nucleus is located at the base of the cell. Unlike the type A gland cells the boundaries of the type B cells are clearly observed.

During the period of the intermolt (Fig. 14a) and the early period of the premolt (D0-1 stages, Fig. 14b), each SE cell possesses a small-dense centrally placed nucleus. The cytoplasm is not stained with PAS. Both types of tegumental glands are present. The period from the early premolt (D2 stage, Fig. 14c) to the early postmolt stage (A stage, Fig. 14d), the SE cells are easily recognized, as the cytoplasm is positively stained with PAS (also stains red with Ponceau S, Fig. 14f), while the nucleus is enlarged and lightly stained. The tegumental glands increase in both size and numbers. In the late postmolt (late B stage), the numbers of PAS stained SE cell dramatically decreases and the tegumental glands show a dramatic decrease in both size and number (Fig. 14e).

Discussion.

1. Determination of the molting stages.

An accurate and consistent determination of the molting stages is essential for the study of the molting cycle. Many criteria have been used by other workers for the precise determination of the molting stages of various crustaceans (for review, see Promwikorn *et al.*, 2004). In this work we have used both physical and histological criteria of the cuticular tissue to determine the molting stages of the black tiger shrimp. The physical criteria have been modified from the criteria described for the brachyuran *Cancer pagurus* by Drach (1939), and the histological criteria have been modified from what Skinner (1962) described for the land crabs *Gecarcinus lateralis* (Stevenson, 1985). Each method has its own advantages and disadvantages. Physical examination is a quick and non-lethal method. We used the degree of retraction of the epidermal tissue from the cuticle, the width of the clear zone between the setal cones and the epidermis, the characteristics of the epidermis, the presence of newly-formed setae and the formation of setal cones as the criteria for molt staging. This method is suitable for distinguishing molting stages in live shrimps, especially for the premolt stage that is composed of D1, D2, D3, and D4 sub-stages, and the early postmolt stages including A1, A2, and B1 sub-stages. In these stages the cuticular tissue develops unique characteristics. We use this method for daily determination of the molting stages. However, this method is not suitable for distinguishing the late postmolt and intermolt stages, including B2, C1, C2, C3 and C4, as in these stages the differences of the physical characteristics of the cuticular tissue are difficult to observe. Histological examination of the cuticle is therefore introduced as an additional method for distinguishing the premolt, postmolt and intermolt stages based on the characteristics and texture of the cuticular tissue. After PAS and hematoxyllin staining, each of the four layers from exterior to interior, an epicuticle, an exocuticle, an endocuticle and a membranous layer show consistent changes and develop unique characteristics. A new epicuticle and exocuticle are synthesised during the period of the late premolt (D3-D4 stages). Thus the epicuticle and exocuticle are so-called pre-ecdysial layers. A new endocuticle and membranous layer are synthesised during the period of the postmolt (A-B-C1-2 stages). Hence, the endocuticle and membranous layer are so-called post-ecdysial layers. This method is suitable for differentiating the late postmolt stage (B2-C1-C2 stages) from the intermolt stage (C3-C4 stages). Only the cuticle of the shrimp intermolt stage has all the cuticular layers, while the cuticle of the shrimp at the postmolt stage has no membranous layer.

However, this method is not suitable for distinguishing the early premolt sub-stages (D1, D1 and D2 stages) and the late postmolt sub-stages (B2, C1 and C2 stages) from each other. In short, physical and histological methods have their-own advantages and disadvantages. Application of both methods has helped us to accurately and consistently identify the molting stages for *Penaeus monodon*.

2. Changes in epidermal cell morphology throughout the molting cycle.

The morphology of the epidermal cells changes actively throughout the molting cycle. Two types of epidermal cells are organized into a single cell layer underneath the cuticle. The major type is named the type I epidermal cell, and the minority type is named the type II epidermal cell. In the intermolt stage, the epidermal cells, in general, are short and arranged untidily. During the period of the premolt stages, the epidermal cells increase in cell height and number, and reorganize into a tidy row. These events occur simultaneously with the appearance of a newly synthesized pre-ecdysial layer underneath the old cuticle. After ecdysis, the epidermal cell height gradually decreases concurrently with the synthesis of the post-ecdysial layer. When the molting stage returns to the intermolt stages (C3-C4 stages), the cell height is least, while the cuticular regeneration is completed. This indicates that the epidermal cell height increases during the period of active cuticular regeneration. We suggest that the early premolt period (D2 stage) is the time when the epidermal cells prepare for cuticular synthesis. The late premolt (D3 and D4 stages) to the postmolt (A1, A2, B1, B2, C1 and C2) period is the time taken for generation of the pre- and post-ecdysial layer. Because of the synthesis of the new cuticle the cells increase intracellular activities, such as DNA replication, RNA transcription, protein synthesis, calcium dynamics as reported in other crustacean species (Skinner, 1966; McWhinnie and Mohrherr, 1970; Humphreys and Stevenson, 1973; Wittig and Stevenson, 1975; Dall and Barclay, 1979; Wheatly et al., 2002; Ahearn et al., 2004; Luquet and Marin 2004). The increase of intracellular activities leads to the increase of cell height. When the rate of synthesis of the new cuticle decreases after ecdysis, especially at the mid postmolt stage (B), the cell height gradually decreases. This indicates the onset of down-regulation of cellular activities. Finally when the cuticular regeneration process is completed in the intermolt stage, the epidermal cell activities are at their lowest level and the cells have their shortest height. A similar pattern of epidermal change has been previously observed, and described for other crustaceans (for example; Skinner, 1966; Green and Neff, 1972; Schultz and Kennedy, 1977).

There has been no previous report about the type II epidermal cells in other species. We find that the epidermal cells of type II stain palely with modified Masson's trichrome, but are positively stained with PAS. An increase in number is observed during the early premolt (D2 stage) to the early postmolt period (A stage). The evidence shows that this cell connects to the epicuticle with cytoplasmic extensions that pass through the canal that forms across the cuticle. These results indicate that the cytoplasmic extensions of the type II epidermal cell may be related to the movement of carbohydrate to the newly synthesized cuticle, especially the epicuticle.

It is concluded that the cellular activities determine the height of the type I epidermal cell. Cellular activities change in relation to the progression of the molting cycle. They start to increase during the early premolt stage (D0), reach a maximum height during the mid premolt (D2) to early postmolt (A) stages, and thereafter gradually decline towards the intermolt stage, in accord with the active period of cuticular regeneration.

3. Ultra-structural differences of the epidermal cells during the molting cycle.

Two types of epidermal cells are observed; the majority and the minority cells, the latter scattered rarely and randomly between the former. We might expect that these 2 types would correspond to the type I and type II cells observed in the LM findings. The ultra-structures of the type I epidermal cell varies depending on the stage of the molting cycle. These variations include reorganization of the cells, shape and size of the cell and nucleus, number of mitochondria, RER, free ribosomes, secretory vesicles, method of secretion, cytoplasmic extensions and development of extracellular spaces around the epidermal cell.

The epidermal cell changes from a tall columnar shape in the premolt stage to a short and irregular shape in the intermolt stage. This occurs concurrently with a decrease in the amount of RER, free ribosomes and mitochondria. This indicates that the cell is mainly responsible for protein and energy production during progression of the molting cycle. Protein production and energy consumption are in greatest demand during the period just before and after ecdysis, and in less demand when the synthesis of the cuticle is complete. Apart from the above organelles, the cell possesses many micro-fibers, and secretory vesicles and granules. This confirms that the fibers and vesicles should be part of the protein products generated by the epidermal cell. Energy from the numerous mitochondria should help in the transport of

these protein products. The presence of a euchromatic nucleus during all molting stages indicates that the cell is active at all times, even in the intermolt stage. During the intermolt stage the cell may still have some activities running to prepare for the next molting cycle.

The methods of pre-ecdysial and post-ecdysial cuticle secretion are different. The micro-fibers, which are arranged into bundles originating within the apical cytoplasm of the type I epidermal cells directly pierce into the newly secreted cuticle during the premolt stage. The electron-dense and electron-translucent secretory vesicles are exported by exocytosis through the top of the cells during the premolt and postmolt stages, respectively. The electron-dense vesicles are directly secreted into the new cuticle, but the electron-translucent vesicles are first secreted into the apical space, helped by the cellular extensions, before being incorporated into the new cuticle through small paths appearing at the lower margin of the new cuticle. This raises the question, why do cell extensions and apical spaces exist only in the postmolt stage? We suggest two reasons. Firstly, a huge export of post-ecdysial secretory vesicles is required, so the cell develops cytoplasmic extensions in order to increase its surface area to allow for this massive exocytosis. Hence the function of these cytoplasmic extensions should be equivalent to that of microvilli. It has been previously reported that the midgut epithelium of a terrestrial crustacean, *Orchestia cavimana*, develops microvilli during the postmolt period (Hecker *et al.*, 2004). We think this should be a similar case. Secondly, the apical space should serve as a site for gathering or mixing materials from the cells and intercellular spaces before being incorporated into the new cuticle. These materials could be both organic and inorganic. From the results, we suggest that the materials needed for the synthesis of new pre-ecdysial and post-ecdysial cuticles should be different. Potential materials required for the pre-ecdysial cuticle include micro-fibers and electron-dense secretory vesicles, while the material for the post-ecdysial cuticle is present in the electron-translucent secretory vesicles. Hence the pre-ecdysial cuticle should have a strong infrastructure, which serves as an external protective shield for the animal. The post-ecdysial cuticle, which is only composed of protein granules, should have a more delicate texture, which reinforces the function of the pre-ecdysial layer, but is suitable for being located interiorly. This does not include the deposition of inorganic materials which are found in most layers of the cuticle (Stevenson, 1985; Pratoomchat *et al.*, 2002a). The slim band, appearing between the epidermal cells and the cuticle in the intermolt stage, could indicate firm attachment of the cells to the cuticle, and imply the ending of the process of cuticle formation.

Dilated extracellular spaces are found around an epidermal cell. Dilated intercellular spaces are observed during the late premolt to intermolt, basal spaces during the premolt period and apical spaces during the postmolt stages. Apical, lateral and basal cell extensions are found together with collections of electron-dense granules/precipitations in these spaces. A similar finding has been previously observed, at the anterior sternum of the terrestrial isopod *Porcellio scaber* (Crustacea) during the re-absorption of calcium carbonate (Ziegler, 1996) when apical cell extensions, an interstitial network and electron-dense granules are found in the cytoplasm and epithelium. It is suggested that these structures could be responsible for the re-absorption and secretion of organic and inorganic materials from and to the cuticle (Roer and Dillaman, 1984; Machado *et al.*, 1990; Compere *et al.*, 1993; Ziegler, 1996; Hagedorn and Ziegler, 2002; Pratoomchat *et al.*, 2002a). The calcium is transported by either trans-epidermal cells or through paracellular spaces between the epidermal cells to reach the haemolymph (Ziegler, 1996; Wheatly *et al.*, 2002; Ahearn *et al.*, 2004; Luquet and Marin 2004). The finding of orchestin, a calcium-binding phosphoprotein, in the intercellular space and in the cytoplasm of the midgut epithelium of *O. cavimana* during the postmolt period (Hecker *et al.*, 2004) supports the previous suggestion. It is noted that the intercellular space especially has many groups of round electron-dense granules at the late premolt stage. We are still unclear what the groups of round electron-dense granules might be, and how they are related to the molting cycle. They could be some pigments, inorganic materials, or something else, that could be closely related to the haemolyphatic sinus.

The characteristics of the type II epidermal cell are clearly different from those of the type I cell. The type II epidermal cells have a euchromatic nucleus, numerous electron-dense vesicles, a large number of free ribosomes, apical cytoplasmic processes and a few mitochondria. We suggest that in relation to the ultrastructures the type II epidermal cell should be responsible mainly for protein production. The cytoplasmic processes may help in the secretion of cellular products and should be the parts inserted into the pore canal in the cuticle as seen from LM evidence. Taken together with the LM result, it indicates that the type II epidermal cell produces not only carbohydrate, but also protein needed for new cuticle regeneration. This material is probably in a modified form such as a glycoprotein that corresponds to LM findings that shows the deposition of carbohydrate and protein in the epicuticle (Figs. 4, 5). This cell has no micro-fibers in the cytoplasm, which explains its inability to stain with the modified trichrome staining.

We conclude that the variations in cytoplasmic content, secretory methods, the width of the intercellular spaces and cell extensions during the premolt and postmolt stages indicate that each of the epidermal cell types play different roles in the synthesis of the pre-ecdysial and post-ecdysial cuticles.

4. Changes in carbohydrate and protein deposition in the sub-epidermis.

As the cytoplasm of the SE cell, stained pink with PAS, and red with Ponceau S, this indicates that carbohydrate and protein (possibly in modified forms) are present in the cytoplasm. It has been previously shown that with other crustaceans, not shrimp, the sub-epidermal tissue stores lipoprotein and carbohydrate for the developing cuticle (Travis, 1955; Skinner, 1962; Green and Neff, 1972; Babu *et al.*, 1985). We found that changes occurred in carbohydrate and protein depositions in the sub-epidermis during the molting cycle. The number of PAS stained SE cell varies throughout the molting cycle with high numbers from the early premolt (D2) to early postmolt (A) stages, low numbers in the late postmolt (B) stages, and very few during intermolt to early premolt (D0-1) stages. This finding implies that the storage of carbohydrate and protein in the sub-epidermis apparently increases during the period of early premolt to early postmolt stages, decreases in late postmolt stages, and is absent during intermolt to early premolt stages. The degree of carbohydrate and protein storage corresponds to the active period of new cuticle regeneration. This correlation indicates that carbohydrate and protein in the SE cell serve as the store for the regeneration of new cuticle. Carbohydrate and protein stored in the sub-epidermis are possibly transported through the epidermis, and finally incorporated into the developing cuticle. It is noted that the type II epidermal cell may be involved in the secretory pathway of carbohydrate, as it is stained pink by PAS and also increases in numbers during the active period of cuticular regeneration.

It is noteworthy that in other crustacean species, many types of tegumental glands can be found in the sub-epidermis (Stevenson 1985). However, details of those glands have not been clearly described. In our experiment we find two obvious types (A and B) of tegumental glands after PAS staining. Type A tegumental gland is stained pink with PAS. It also shows numerous secretory granules, which stain with toluidine blue. Type B tegumental gland is stained less intensely with PAS, and contains mucus in the cytoplasm. It also shows a metachromasia reaction, when it is stained with toluidine blue. These results suggest that both

tegumental glands contain carbohydrate. Type B tegumental gland also contains mucus and substances causing metachromasia reaction such as histamine, heparin, etc. In other species the tegumental glands contain phenoloxidase (Stevenson, 1961), tyrosinase (Stevenson and Schneider, 1962), and mucopolysaccharides (Dall, 1965; Stevenson and Murphy, 1967; Shyamasundari and Hanumantha, 1978). Increases in the quality and quantity of both glands during the early premolt to early postmolt period indicate a high activity of these glands that corresponds to the active period of cuticular regeneration. These glands should therefore produce some essential materials for the newly synthesized cuticle.

We conclude that the sub-epidermal tissue is the main store of carbohydrate, protein, mucous and other essential substances required for the newly synthesized cuticle of the black tiger shrimp.

Concluding remarks.

For the first time, this paper shows the dynamic changes that occur in the epidermal and sub-epidermal structures throughout the molting cycle of the black tiger shrimp. All results point to the conclusion that both the epidermis and sub-epidermis have major roles in cuticular regeneration. We conclude that the major type I epidermal cell, is responsible for the synthesis of protein and micro-fibers. The type II epidermal cell is involved in the synthesis of protein and carbohydrate. The sub-epidermis serves as a store of carbohydrate, protein, mucus and other unidentified substances. The period of the early premolt (D0-1) is the time when increased cellular activities are initiated. The mid premolt (D2) to early postmolt (A) period is the time of highest cellular activities. During the late postmolt (B-C2) period all cellular activities are down-regulating. Lastly during the intermolt (C3-4) period there is very little metabolic activity in the epidermal tissues.

Acknowledgements.

This work is financially supported by the Thailand Research Fund (MRG4680061). We specially thank Dr. Brian Hodgson for critical proof on the manuscript.

References

1. Aoto TY, Kamiguchi Y, Hisano S. 1974. Histological and ultrastructural studies on the Y-organ and the mandibular organ of the freshwater prawn, *Palomino paucidens*, with special reference to their relations with the molting cycle. *J Fac Sci Hokkaido Univ* 19:295-308.
2. Ahearn GA, Mandal PK, Mandal A. 2004. Calcium regulation in crustaceans during the molt cycle: a review and update. *Comp Biochem Physiol* 137A:247-257.
3. Aragon S, Claudinot S, Blais C, Maibèche M, Dauphin-Villemant C. 2002. Molting cycle-dependent expression of CYP4C15, a cytochrome P450 enzyme putatively involved in ecdysteroidogenesis in the crayfish, *Orconectes limosus*. *Insect Biochem Mol Biol* 32:153-159.
4. Babu DE, Hanumantha RK, Shyamasundari K, Uma Devi DV. 1985. Histochemistry of the cuticle of the crab *Menippe rumphii* (Fabricius) (Crustacea: Brachyura) in relation to moulting. *J Exp Marine Biol Ecol* 88:129-144.
5. Bellon-Humbert C, Van Herp F. 1988. Localisation of serotonin-like immunoreactivity in the eyestalk of the prawn *Palaemon serratus* (Crustacea, Decapoda, Natantia). *J Morphol* 196:307-320.
6. Bielefeld M, Gellissen G, Spindler KD. 1986. Protein production and the moulting cycle in the crayfish *Astacus leptodactylus*-I, stage-specificity of polypeptide patterns in the hypodermis and hepatopancreas. *Insect Biochem* 16:175-180.
7. Borst DW, Ogan J, Tsukimura B, Claerhout T, Holford KC. 2001. Regulation of the crustacean mandibular organ. *Am Zool* 41:430-441.
8. Bancroft JD, Gamble M. 2002a. *Theory and Practice of Histological Techniques*. 5th ed. London: Harcourt publisher limited. 153 p.
9. Bancroft JD, Gamble M. 2002b. *Theory and Practice of Histological Techniques*. 5th ed. London: Harcourt publisher limited. 175 p.
10. Brannon AC, Rao KR. 1979. Barium, strontium and calcium levels in the exoskeleton, hepatopancreas and abdominal muscle of the grass shrimp, *Palaemonetes pugio*: Relation to molting and exposure to barite. *Comp Biochem Physiol* 63A:261-274.
11. Buda ES, Shafer TH. 2005. Expression of a serine proteinase homolog prophenoloxidase-activating factor from the blue crab, *Callinectes sapidus*. *Comp Biochem Physiol* 140B:521-531.

12. Burse CR, Lane CE. 1971. Ionic and protein concentration changes during the molt cycle of *Penaeus duorarum*. *Comp Biochem Physiol* 40A:155-162.
13. Byard EH, Shivers RR, Aiken DE. 1975. The mandibular organ of the lobster, *Homarus americanus*. *Cell Tiss Res* 162:13-22.
14. Cariolou MA, Flytzanis CN. 1994. Differential expression of cuticle-epidermis proteins in the shrimp *Penaeus vannamei* during molting. *Comp Biochem Physiol* 3:367-373.
15. Carlisle DB. 1957. On the hormonal inhibition of moulting in Decapod Crustacea II. The terminal anecdysis in crabs. *J Mar Biol Assoc U.K.* 36:291-307.
16. Chang ES, Chang SA, Mulder EP. 2001. Hormones in the lives of crustaceans: An overview. *Am Zool* 41:1090-1097.
17. Compere P, Morgan JA, Goffinet G. 1993. Ultrastructure location of calcium and magnesium during mineralization of the cuticle of the shore crab, as determined by the K-pyroantimonate method and X-ray microanalysis. *Cell Tissue Res* 274:567-577.
18. Cuzin-Roudy J, Strambi C, Strambi A, Delbecque JP. 1989. Hemolymph ecdysteroids and molt cycle in males and females of *Siriella armata* M.-Edw. (Crustacea: Mysidacea): Possible control by the MI-ME X-organ of the eyestalk. *Gen Comp Endocrinol* 74:96-109.
19. Dall W. 1965. The physiology of a shrimp *Metapenaeus mastersii*. III. Composition and structure of the integument. *Aust J Mar Freshwater Res* 16:13-23.
20. Dall W, Barclay MC. 1979. The effect of exogenous 20-hydroxyecdysone on levels of epidermal DNA and RNA in the western rock lobster. *J Exp Mar Biol Ecol* 36:103-110.
21. Drach P. 1939. Mue et cycle d'intermue chez les crustaces Decapodes. *Annls Inst Oceanogr* 19:103-391.
22. Endo H, Persson P, Watanabe T. 2000. Molecular cloning of the crustacean DD4 cDNA encoding a Ca²⁺-binding protein. *Biochem Biophys Res Commun* 276:286-291.
23. Favrel P, Van Wormhoudt A, Studler JM, Bellon C. 1987. Immunochemical and biochemical characterisation of gastrin/cholecystokinin-like peptides in *Palaemon serratus* (Crustacea Decapoda): intermolt variations. *Endocrinol* 65:363-372.
24. Fernandez-Gimenez AV, Garcia-Carren FL, Navarrete del Toro MA, Fenucci JL. 2001. Digestive proteinases of red shrimp *Pleoticus muelleri* (Decapoda, penaeoidea): Partial characterization and relationship with molting. *Comp Biochem Physiol* 130B:331-338.
25. Fernandez-Gimenez AV, Garcia-Carren FL, Navarrete del Toro MA, Fenucci JL. 2002. Digestive proteinases of *Artemesia longinans* (Decapoda, Penaeidae) and relationship with molting. *Comp Biochem Physiol* 132B:593-598.

26. Freeman JA, Costlow JD. 1979. Hormonal control of apolysis in barnacle tissue epidermis *in vitro*. *J Exp Zool* 210:333-346.
27. Gersch M. 1979. A new endocrine gland in the antennal segment of the crayfishes *Orconectes limosus* and *Astacus astacus*. *Gen Comp Endocrinol* 39:490-497.
28. Glynn JP. 1968. Studies on the ionic, protein, and phosphate changes associated with the moult cycle of *Homarus vulgaris*. *Comp Biochem Physiol* 26:937-946.
29. Graf F, Delbecque JP. 1987. Ecdysteroid titers during the molt cycle of *Orchestia cavimana* (Crustacea, Amphipoda). *Gen Comp Endocrinol* 65:23-33.
30. Gunamalai V, Kirubakaran R, Subramoniam T. 2004. Hormonal coordination of molting and female reproduction by ecdysteroids in the mole crab *Emerita asiatica* (Milne Edwards). *Gen Comp Endocrinol* 138:128-138.
31. Green JP, Neff MR. 1972. A survey of the fine structure of the integument of the fiddler crab. *Tissue Cell* 4:137-171.
32. Hagedorn M, Ziegler A. 2002. Analysis of Ca²⁺ uptake into the smooth endoplasmic reticulum of permeabilized sternal epithelial cells during the moulting cycle of the terrestrial isopod *Porcellio scaber*. *J Exp Biol* 205:1935-1942.
33. Hecker A, Quennedey B, Testenièrè O, Quennedey A, Graf F, Luquet G. 2004. Orchestin, a calcium-binding phosphoprotein, is a matrix component of two successive transitory calcified biomineralizations cyclically elaborated by a terrestrial crustacean. *J Struct Biol* 146:310-324.
34. Hinsch GW, Hajj HA. 1975. The ecdysial gland of the spider crab, *Libinia emarginata* (L.). I. Ultrastructure of the gland in the male. *J Morphol* 145:179-187.
35. Homola E, Chang ES. 1997. Methyl farnesoate: Crustacean juvenile hormone in search of functions. *Comp Biochem Physiol*. 117B:347-356.
36. Hubschman JH, Armstrong PW. 1972. Influence of ecdysterone on molting in *Palaemonetes*. *Gen Comp Endocrinol* 18:345-438.
37. Humphreys CR, Stevenson JR. 1973. Changes in epidermal DNA, protein and protein synthesis during the molt cycle of the crayfish *Orconectes sanborni* (Faxon). *Comp Biochem Physiol* 44A:1121-1128.
38. Huner JV, Colvin BL, Reid BL. 1979a. Postmolt mineralization of the exoskeleton of juvenile California brown shrimp, *Penaeus californiensis* (Decapoda: Penaeidae). *Comp Biochem Physiol* 62A:889-893.

39. Huner JV, Colvin BL, Reid BL. 1979b. Whole-body calcium, magnesium and phosphorus levels of the California brown shrimp, *Penaeus californiensis* (Decapoda: Penaeidae) as functions of molt stage. *Comp Biochem Physiol* 64A:33-36.
40. Ikeya T, Persson P, Kono M, Watanabe T. 2001. The DD5 gene of the decapod crustacean *Penaeus japonicus* encodes a putative exoskeletal protein with a novel tandem repeat structure. *Comp Biochem Physiol* 128B:379-388.
41. Keller R, Schmid E. 1979. *In vitro* secretion of ecdysteroids by Y-organs and lack of secretion by mandibular organs of the crayfish following molt induction. *J Comp Physiol* 130:347-353.
42. Keller R, Willig A. 1976. Experimental evidence of the molt controlling function of the Y-organ of a macruran decapod, *Orconectes limosus*. *J Comp Physiol* 108:271-278.
43. Lipcius RN, Herrnkind WF. 1982. Molt cycle alterations in behavior, feeding and diel rhythms of a decapod crustacean, the spiny lobster *Panulirus argus*. *Mar Biol* 68:241-252.
44. Luquet G, Marin M. 2004. Biomineralisations in crustaceans: storage strategies. *Gen Paleontol* 3:515-534.
45. Machado J, Ferreira KG, Ferreira HG, Fernandes PL. 1990. The acid-base balance mantle epithelium *Anodonta cygnea*. *J Exp Zool* 150:159-169.
46. McWhinnie MA, Mohrherr CJ. 1970. Influence of eyestalk factors, intermolt cycle and season upon ¹⁴C-leucine incorporation into protein in the crayfish (*Orconectes virilis*). *Comp Biochem Physiol* 34:415-437.
47. Mercaldo-Allen R. 1991. Changes in the blood chemistry of the American lobster, *Homarus americanus*, H. Milne Edwards, 1837 over the molt cycle. *J Shellfish Res* 10:147-156.
48. Meunpol O, Hall MR, Kapoor V. 1998. Partial characterization and distribution of kynurenine aminotransferase activity in the black tiger prawn (*Penaeus monodon*). *Comp Biochem Physiol* 120B:139-143.
49. Miyawaki M, Taketomi Y. 1984. The microvilli of the midgut epithelium in the freshwater shrimp, *Caridina denticulata*. *Cell Biol Intl Rep* 8:265-268.
50. Morgan GR. 1978. Locomotor activity in the western rock lobster, *Panulirus longipes cygnus*. *Austr J Mar Freshwater Res* 29:169-174.
51. Nagaraju GPC, Reddy, PR, Reddy PS. 2004. Mandibular organ: it's relation to body weight, sex, molt and reproduction in the crab, *Oziotelphusa senex senex fabricius* (1791). *Aquaculture* 232:603-612.

52. Nakatsuji T, Sonobe H. 2004. Regulation of ecdysteroid secretion from the Y-organ by molt-inhibiting hormone in the American crayfish, *Procambarus clarkii*. *Gen Comp Endocrinol* 135:358-364.
53. Pratoomchat B, Sawangwong P, Guedes R, De Iurdes Reis M, Machado J. 2002b. Cuticle ultrastructures changes in the crab *Scylla serrata* over the molt cycle. *J Exp Zool* 293:414-426.
54. Pratoomchat B, Sawangwong P, Pakkong P, Machado J. 2002a. Organic and inorganic compound variations in haemolymph, epidermal tissue and cuticle over the molt cycle in *Scylla serrata* (Decapoda). *Comp Biochem Physiol* 131A:243-255.
55. Promwikorn W, Kirirat P, Thaweethamseewee P. 2004. Index of molting cycle in the black tiger shrimp (*Penaeus monodon*). *Songklanakarin J Sci Technol* 26:765-772.
56. Promwikorn W, Boonyoung P, Kirirat P. 2005. Histological characterization of cuticular depositions throughout the molting cycle of the black tiger shrimp (*Penaeus monodon*). *Songklanakarin J Sci Technol* (in press).
57. Rahman MK, Subramoniam T. 1989. Molting and its control in the female sand lobster *Thenus orientalis* (Lund). *J Exp Mar Biol Ecol* 128:105-115.
58. Rao KR, Fingerma M, Fingerma SW. 1973. Effects of exogenous ecdysones on the molt cycles of fourth and fifth stage American lobsters, *Homarus americanus*. *Comp Biochem Physiol* 44A:1105-1120.
59. Roer R, Dillaman R. 1984. The structure and calcification of the crustacean cuticle. *Amer Zool* 24:893-909.
60. Schultz TW, Kennedy JR. 1977. Analyses of the integument and muscle attachment in *Daphnia pulex* Cladocera Crustacea. *J Submicrosc Cytol* 9:37-51.
61. Scott-Fordsmand JJ, Depledge MH. 1997. Changes in the tissue concentrations and contents of calcium, copper and zinc in the shore crab *Carcinus maenas* (L.) (Crustacea: Decapoda) during the moult cycle and following copper exposure during ecdysis. *Mar Env Res* 44:397-414.
62. Shyamasundari K, Hanumantha RK. 1978. Studies on the Indian sand lobster *Thenus orientalis*. Mucopolysaccharides of the tegumental glands. *Folia Histochem Cytochem* 16:247-254.
63. Skinner DM. 1962. The structure and metabolism of a crustacean integumentary tissue during a molt cycle. *Biol Bull* 123:635-647.

64. Skinner DM. 1966. Macromolecular changes associated with the growth of crustacean tissues. *Am Zool* 6:235-242.
65. Soumoff C, O'Connor JD. 1982. Repression of Y-organ secretory activity by molt inhibiting hormone in the crab *Pachygrapsus crassipes*. *Gen Comp Endocrinol* 48:432-439.
66. Sousa LG, Petriella AM. 2001. Changes in the hepatopancreas histology of *Palaemonetes argentmus* (Crustacea, Caridea) during moult. *Bio cell* 25:275-281.
67. Spaziani E, Mattson M, Wang WL. 1999. Signaling pathways for ecdysteroid hormone synthesis in crustacean Y-organs. *Am Zool* 39:496-512.
68. Spindler KD, Hennecke R, Gellissen G. 1992. Protein production and the molting cycle in the crayfish *Astacus leptodactylus* (Nordmann, 1842). *Gen Comp Endocrinol* 85:248-253.
69. Stevenson JR. 1961. Polyphenol oxidase in the tegumental glands in relation to the molting cycle of the isopod crustacean *Armadillidium vulgare*. *Bio Bull* 121:554-560.
70. Stevenson JR., Schneider RP. 1962. Tyrosinase activity of organs containing tegumental glands in the crayfish. *J Exp Zool* 150:17-25.
71. Stevenson JR. 1985. Dynamics of the integument. In: Bliss DE, Mantel LH, editor. *The biology of crustacea*, vol. 9. New York: Academic Press. p 1-42.
72. Stevenson JR, Guckert RH, Cohen JD. 1968. Lack of correlation of some proecdysial growth and developmental processes in the crayfish. *Biol Bull* 134:160-175.
73. Stevenson JR, Murphy JC. 1967. Mucopolysaccharide glands in the isopod crustacean *Armadillidium vulgare*. *Trans Am Micros Soc* 86:50-57.
74. Taketomi Y, Hyodo M. 1986. The Y organ of the crab, *Portunus trituberculatus*: Effects of ecdysterone on the ultrastructure. *Cell Biol Intl Rep* 10:367-374.
75. Tamm G, Cobb J. 1978. Behavior and the crustacean molt cycle: changes in aggression of *Homarus americanus*. *Science* 200:79-81.
76. Terwilliger NB, Dancott L, Ryan M. 1999. Cryptocyanin, a crustacean molting protein: Evolutionary link with arthropod hemocyanins and insect hexamerins. *Proc Natl Acad Sci* 96:2013-2018.
77. Terwilliger NB, Otoshi B. 1994. Cryptocyanin and hemocyanin: fluctuations and functions of crab hemolymph proteins during molting. *Am Zool* 37:67A.
78. Teshima SI, Ceccaldi HJ, Patrois J, Kanazawa A. 1975. Bioconversion of desmosterol to cholesterol at various stages of molting cycle in *Palaemon serratus* Pennant, Crustacea, Decapoda. *Comp Biochem Physiol* 50:485-489.

79. Traub M, Gellissen G, Spindler KD. 1987. 20-(OH)-ecdysone-induced transition from intermolt to premolt protein biosynthesis patterns in the hypodermis of the crayfish, *Astacus leptodactylus*, in vitro. *Gen Comp Endocrinol* 65:469-477.
80. Travis DF. 1955. The molting cycle of the spiny lobster *Panulirus argus* Latreille. II. Pre-ecdysial histological and histochemical changes in the hepatopancreas and integumental tissues. *Biol Bull* 108:88-112.
81. Ueno M, Bidmon HJ, Stumpf WE. 1992. Ponasterone-A binding sites in hypodermis during the molting cycle of crayfish *Procambarus clarkii*. *Acta Histochem Cytochem* 25:505-510.
82. Walgraeve HR, Criel GR, Sorgeloos P, De Leenheer AP. 1988. Determination of ecdysteroids during the moult cycle of adult *Artemia*. *J Insect Physiol* 34:597-602.
83. Wang WN, Wang AL, Wang DM, Wang LP, Liu Y, Sun RY. 2003. Calcium, Phosphorus and adenylate levels and Na⁺-K⁺-ATPase activities of prawn, *Macrobrachium nipponense*, during the moult. *Comp Biochem Physiol* 134A:279-305.
84. Watanabe T, Kono M. 1997. Isolation of a DNA encoding a chitinase family protein from cuticular tissues of the Kuruma prawn *Penaeus japonicus*. *Zoolog Sci* 14:65-68.
85. Watanabe T, Persson P, End H, Kono M. 2000. Molecular analysis of two genes, DD9A and B, which are expressed during the postmolt stage in the decapod crustacean *Penaeus japonicus*. *Comp Biochem Physiol* 125:127-136.
86. Watson RD, Spaziani E. 1985. Biosynthesis of ecdysteroids from cholesterol by crab Y-organs, and eyestalk suppression of cholesterol uptake and secretory activity, in vitro. *Gen Comp Endocrinol* 59:140-148.
87. Wheatly MG, Zanutto FP, Hubbard MG. 2002. Calcium homeostasis in crustaceans: subcellular Ca dynamics. *Comp Biochem Physiol* 132B:163-178.
88. Wittig K, Stevenson JR. 1975. DNA synthesis in the crayfish epidermis and its modification by ecdysterone. *J Comp Physiol* 99:279-286.
89. Yudin AI, Diener WH, Clark J, Chang ES. 1980. Mandibular gland of the blue crab, *Callinectes sapidus*. *Bio Bull* 159:760-772.
90. Ziegler A. 1996. Ultrastructural evidence for transepithelial calcium transport in the anterior sternal epithelium of the terrestrial isopod *Porcellio scaber* (Crustacea) during the formation and resorption of CaCO₃ deposits. *Cell Tissue Res* 284:459-466.

Figure legends

Figure 1 Determination of molting stages. Uropods of live black tiger shrimps were examined and photographed under a light microscope (Olympus BX51) connected to a digital camera (Olympus DP11). The criteria used for molt staging were modified from Drach's staging. The images of physical characteristics indicate intermolt stage (a), premolt stage (b-f) and postmolt stage (g, h). EE, epidermal edge; I, indent pattern of the epidermis; L, white layer at the edge of the epidermis; S, setae; SC, setal cone; SCn, newly-formed setal cones; Sn, newly-formed seta; ► = wavy edge of epidermis; * = clear zone between cuticle and epidermis. Bar = 50 μ m.

Figure 2 An exuviae of the black tiger shrimp. Exuviae or old exoskeleton of shrimp was separated into 2 part. The first main part (A) was composed of intact cuticle of the ventral part of the head, trunk, tail and all appendages. The second part (B) was composed of the carapace and rostrum. The images were photographed with a digital camera (Pentax Optio). Bar = 2 cm.

Figure 3 Timing of the molting cycle. Duration of each molting stage during shrimp culture was recorded and presented in a diagram.

Figure 4 Histological criteria for molt staging. The cuticles of the black tiger shrimps in different molting stages were fixed with Davidson's fixative, de-hydrated in increasing concentrations of ethanol, embedded in paraffin. 5 μ m thick paraffin sections were stained with PAS. The images of the cuticle in different molting stages were photographed by a digital camera (Olympus DP11) connected to a light microscope (Olympus BX51). Ed, endocuticle layer; Ep, epicuticle layer; Ex, exocuticle layer; Ml, membranous layer; nEp, new epicuticle layer; nEx, new exocuticle layer; oEp, old epicuticle layer; oEx, old exocuticle layer; nCu, newly synthesized cuticle. Bar = 10 μ m.

Figure 5 Changes of epidermal morphology through the molting cycle. Intact cuticular tissue from the trunk of the black tiger shrimps in various molting stage were fixed with Davidson's fixative, de-hydrated in increasing concentrations of ethanol, embedded in paraffin. 5 μ m thick paraffin sections were stained with modified Masson's trichromes. The images of epidermis and cuticle in different molting stages were photographed by a digital camera (Olympus DP11) connected to a light microscope (Olympus BX51). C, cuticle; E, epidermis, II; epidermal cell type II. Bar = 10 μ m.

Figure 6 The morphology of type I and II epidermal cells. Cuticular tissues of the black tiger shrimps in each molting stage were fixed with Davidson's fixative, de-hydrated in increasing concentrations of ethanol, embedded in paraffin. 5 μm thick paraffin sections were either stained with PAS (a, c), or Masson's trichrome (b). The images of type I and II epidermal cells were photographed by a digital camera (Olympus DP11) connected to a light microscope (Olympus BX51). C, cuticle; I, type I epidermal cell; II, type II epidermal cell; arrow = canal across the cuticle. Bar = 10 μm .

Figure 7 Ultra-structures of epidermal cells. Epidermis from the premolt (D2 stage) was fixed with 2.5% glutaraldehyde and 4% paraformaldehyde for 48 h, and subsequently processed for TEM. The samples were sectioned with an ultra-microtome (MTXL, RMC) with a 60 – 90 nm thickness. Type I and II epidermal cell shows different characteristics. The image was photographed with an electron microscope (Jeol JEM-100 CX II). C, cuticle; EC I, epidermal cell type I; EC II, epidermal cell type II; arrow = micro-fibers. Bar = 4 μm .

Figure 8 Ultra-structures of type I epidermal cell in D2-D3 stages. The epidermis from premolt D2 stage (Fig. 8a, b, d, e) and D3 stage (Fig. 8c) were fixed with 2.5% glutaraldehyde and 4% paraformaldehyde for 48 h, and subsequently processed for TEM. The samples were sectioned with an ultra-microtome (MTXL, RMC) with a 60 – 90 nm thickness. The ultra-structures of type I epidermal cell at various regions were photographed with an electron microscope (Jeol JEM-100 CX II). C, cuticle; F, micro-fibers; M, mitochondria; N, nucleus; RER, rough endoplasmic reticulum. The scales are as indicated in the individual pictures.

Figure 9 Ultra-structures of type I epidermal cell in D4 stage. Epidermis from the late premolt D4 stage was fixed with 2.5% glutaraldehyde and 4% paraformaldehyde for 48 h, and subsequently processed for TEM. The samples were sectioned with an ultra-microtome (MTXL, RMC) with a 60 – 90 nm thickness. The ultra-structures of type I epidermal cell are shown at whole view (a), sub-nuclear (b) and apical (c) regions. Figure 9d shows groups of electron-dense granules locating underneath the epidermal cell layer near the haemolymphic sinus. All images were photographed with an electron microscope (Jeol JEM-100 CX II). BS, basal space; C, cuticle; E, epidermis; F, micro-fibers; G, electron-dense granules; H, haemocyte; HS, haemolymphic space; IS, intercellular space; M, mitochondria; N, nucleus; RER, rough endoplasmic reticulum, * = cytoplasmic protusion. The scales are as indicated in the individual pictures.

Figure 10 Ultra-structures of type I epidermal cell in A stage. Epidermis immediately after molting (postmolt, A stage) was fixed with 2.5% glutaraldehyde and 4%

paraformaldehyde for 48 h, and subsequently processed for TEM. The samples were sectioned with an ultra-microtome (MTXL, RMC) with a 60 – 90 nm thickness. The ultra-structures of type I epidermal cell at apical (a) and middle (b) regions of the cell were photographed with an electron microscope (Jeol JEM-100 CX II). C, cuticle; Et, cell extension; TSV, electron translucent secretory vesicles; V, secretory vesicle; arrowhead = paths connecting between apical space and cuticle. The scales are as indicated in the individual pictures.

Figure 11 Ultra-structures of type I epidermal cell in B stage. Epidermis in late postmolt, Bstage was fixed with 2.5% glutaraldehyde and 4% paraformaldehyde for 48 h, and subsequently processed for TEM. The samples were sectioned with an ultra-microtome (MTXL, RMC) with a 60 – 90 nm thickness. The ultra-structures of epidermal cell type I for whole view (a), and at apical region (b, c) were photographed with an electron microscope (Jeol JEM-100 CX II). AS, apical space; C, cuticle; D, desmosome; Et, cell extension; IS, intercellular space; M, mitochondria; V, secretory vesicle. The scales are as indicated in the individual pictures.

Figure 12 Ultra-structures of intercellular space in various molting stages. Epidermis in the intermolt (a, b), D4 (c), B (d), D2 (e, f) stages were fixed with 2.5% glutaraldehyde and 4% paraformaldehyde for 48 h, and subsequently processed for TEM. The samples were sectioned with an ultra-microtome (MTXL, RMC) with a 60 – 90 nm thickness. The ultra-structures of type I epidermal cell at intercellular space region was photographed with an electron microscope (Jeol JEM-100 CX II). Figure 12b shows overview of intermolt-stage type I epidermal cells. AS, apical space; C, cuticle; D, desmosome; IS, intercellular space; M, mitochondria. The scales are as indicated in the individual pictures.

Figure 13 Ultra-structures of type II epidermal cell. The type II epidermal cell in D2 stage was fixed with 2.5% glutaraldehyde and 4% paraformaldehyde for 48 h, and subsequently processed for TEM. The samples was sectioned with an ultra-microtome (MTXL, RMC) with a 60 – 90 nm thickness. The ultra-structures at apical (a) and middle regions were photographed with an electron microscope (Jeol JEM-100 CX II). CP; cytoplasmic process; M, mitochondria; RER; rough endoplasmic reticulum; V, secretory vesicles. The scales are as indicated in the individual pictures.

Figure 14 Changes of sub-epidermal morphology through the molting cycle. Cuticular tissues of the black tiger shrimps in each stage were either fixed with Davidson's fixative, or 2.5% glutaraldehyde and 4% paraformaldehyde, then processed for paraffin sectioning and

semi-thin sections, respectively. 5 μm thick paraffin sections were stained with PAS (a – e), trichrome (f). The semi-thin sections (1-2 μm thick) were stained with toluidine blue (g, h). The images were photographed by a digital camera (Olympus DP11) connected to a light microscope (Olympus BX51). E, epidermis; Ga, tegumental gland type A; Gb, tegumental gland type B; SE, sub-epidermal cell; Mu, mucus; N, nucleus; ED, excretory duct; arrow = intercellular boundaries, * = metachromasia reaction. Bar = 10 or 15 μm as indicated.

Figure 1

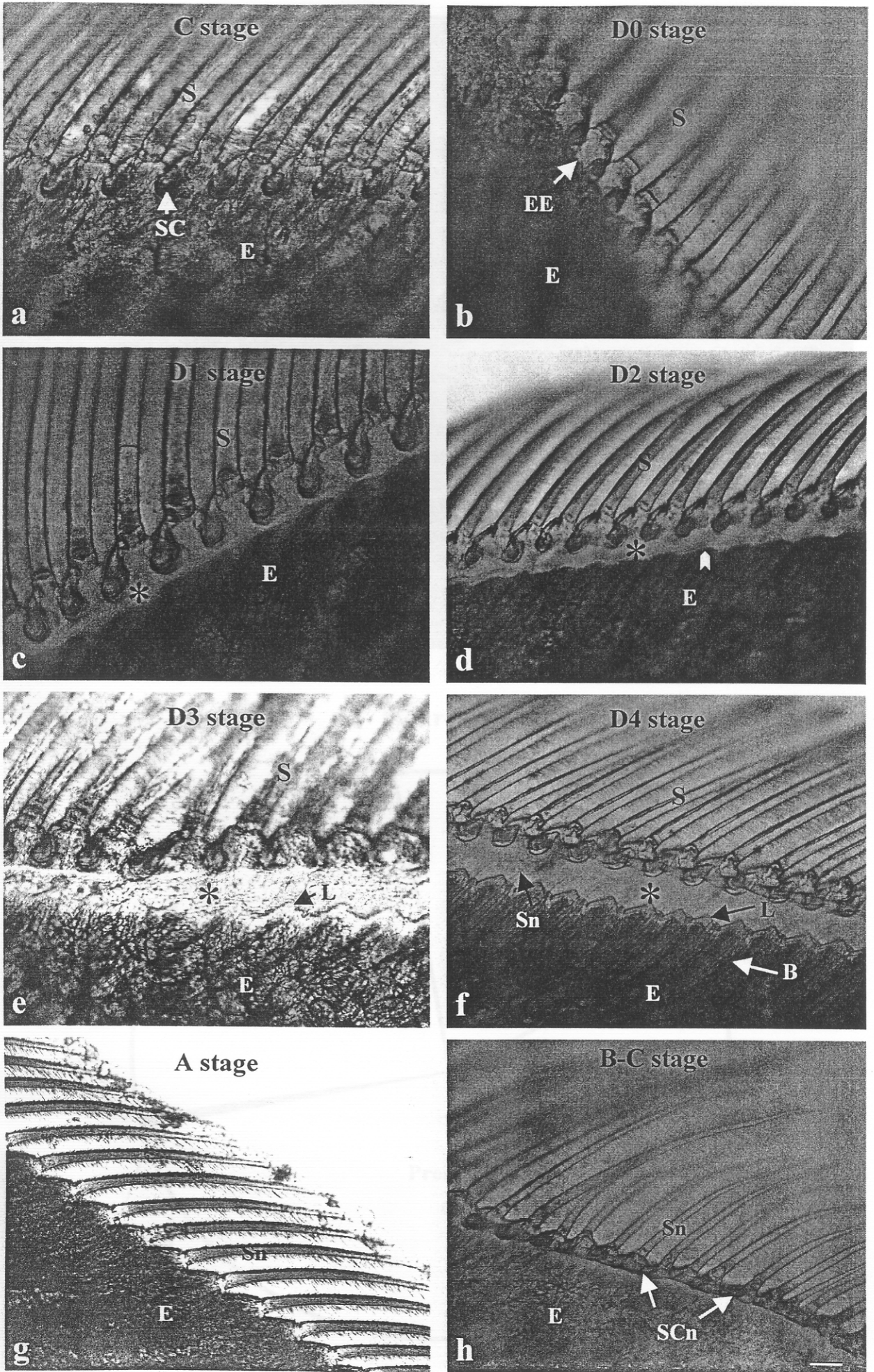


Figure 2

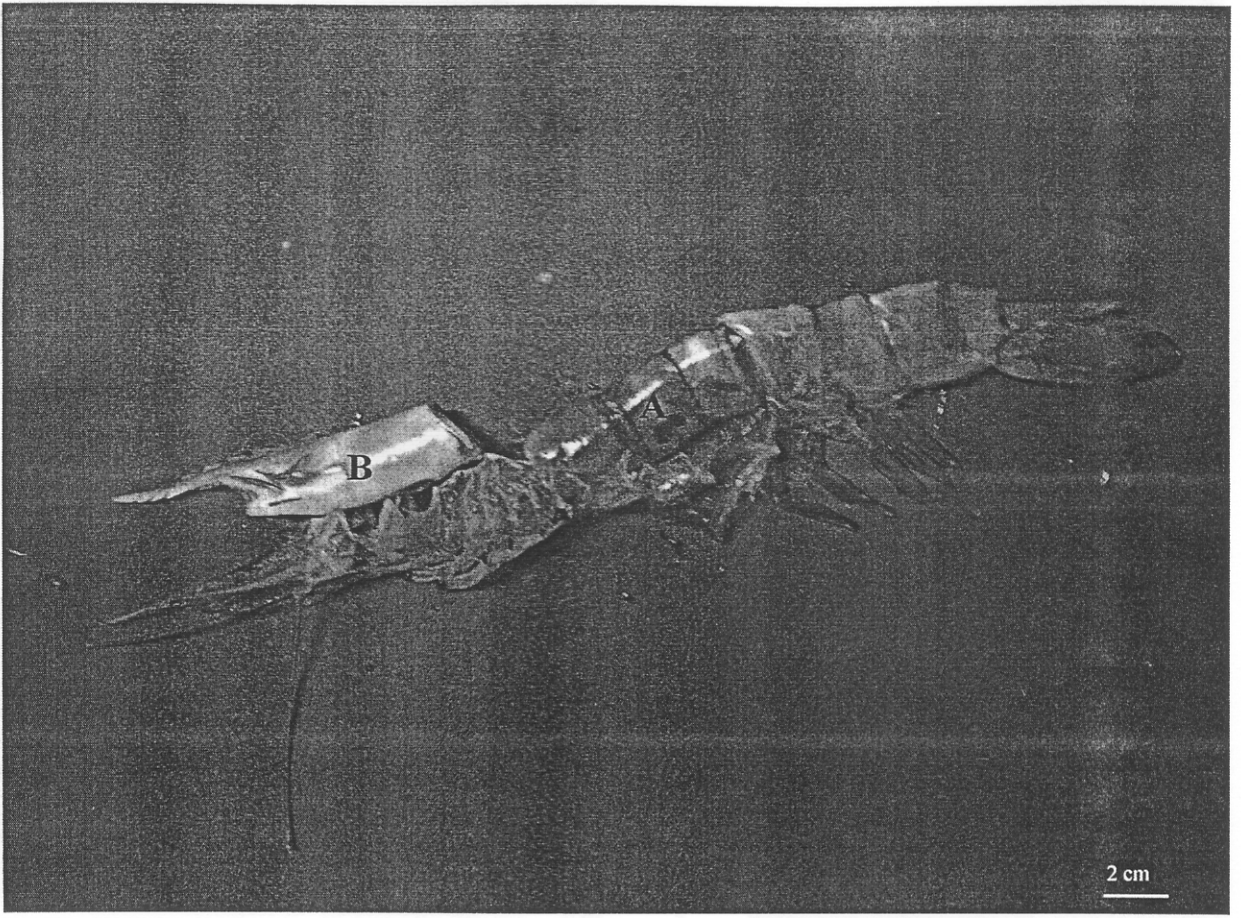


Figure 3

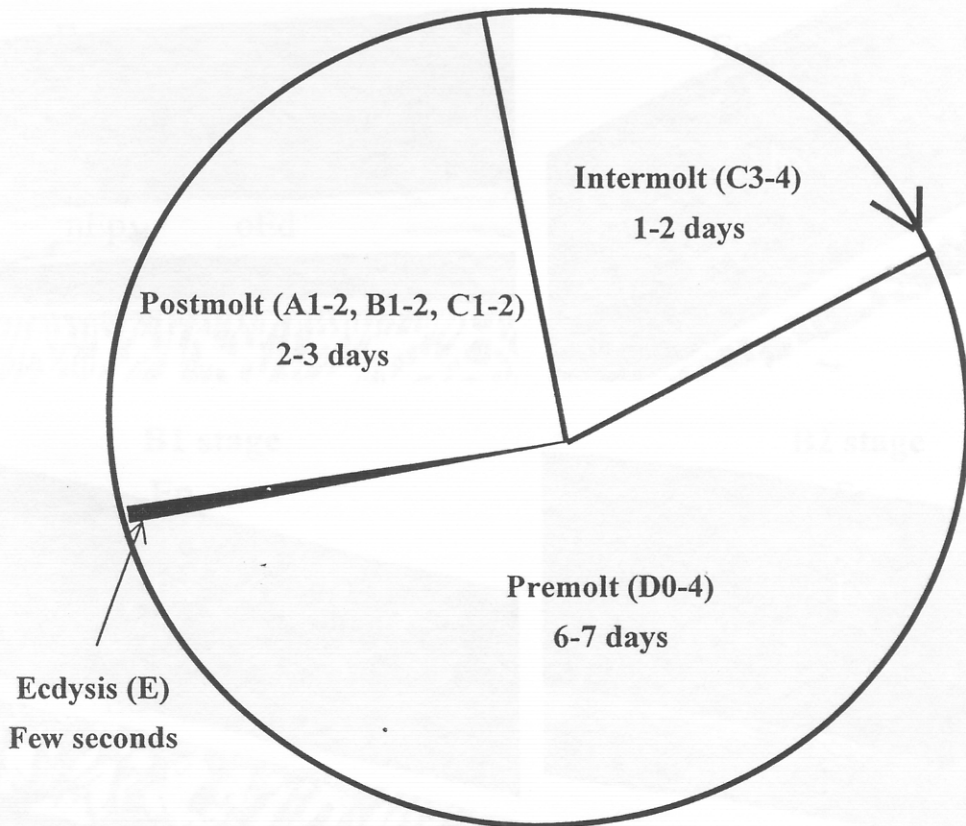


Figure 4

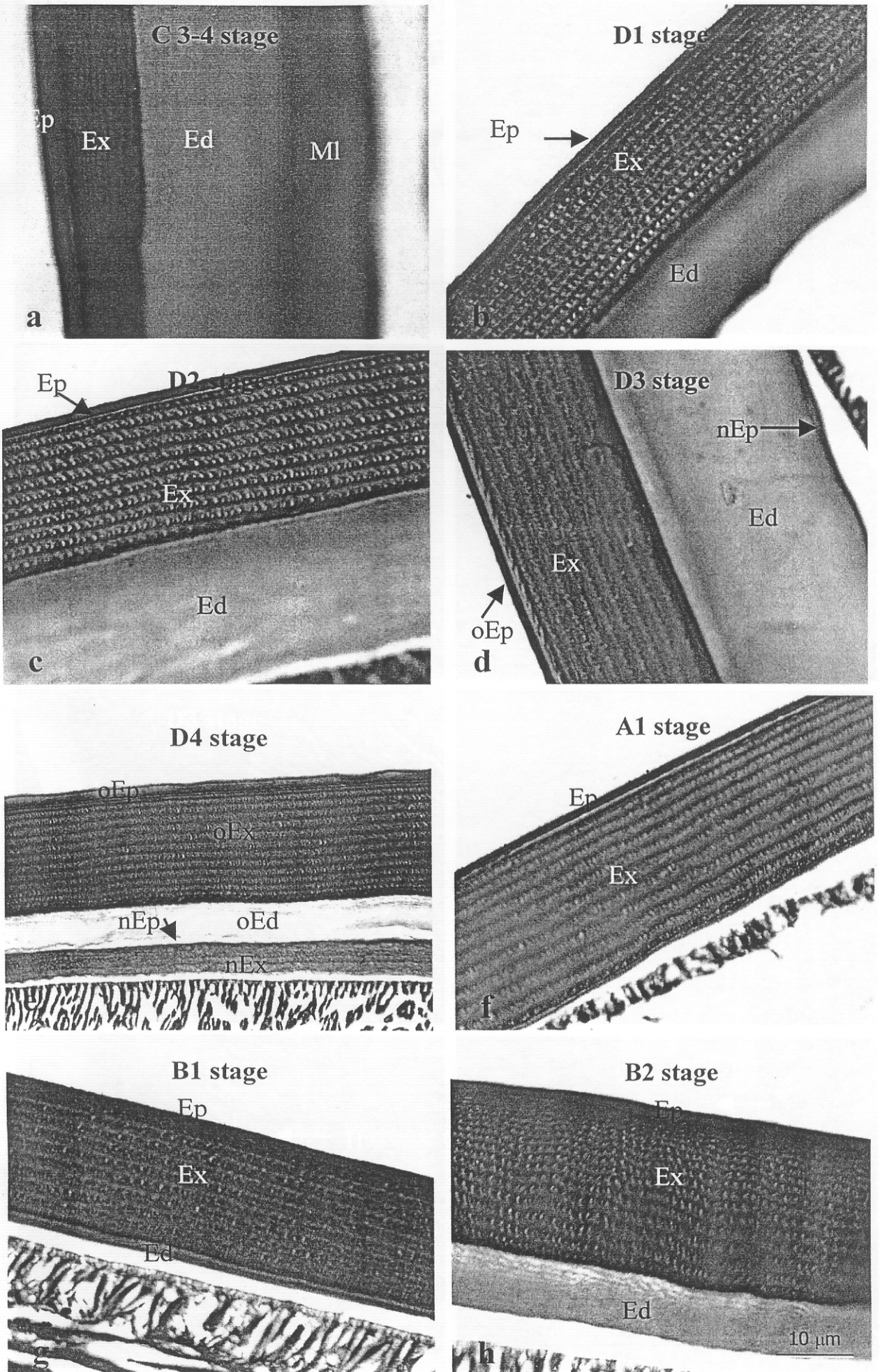


Figure 5

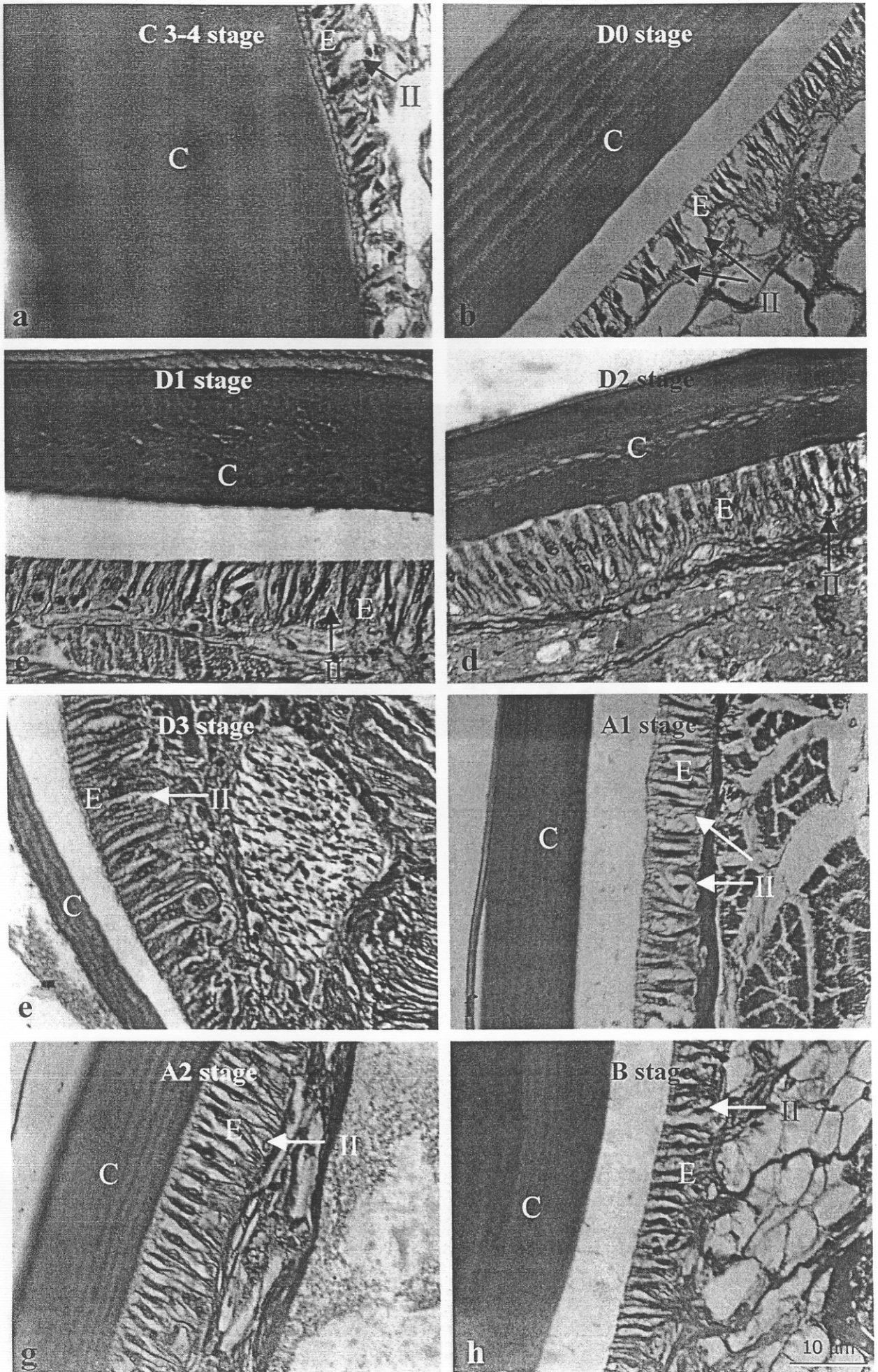


Figure 6

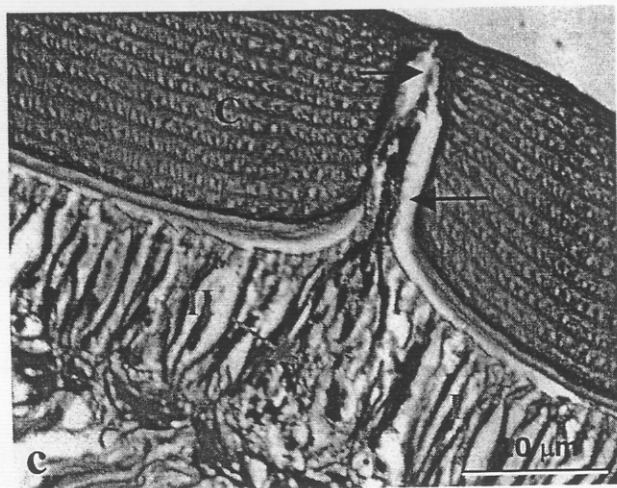
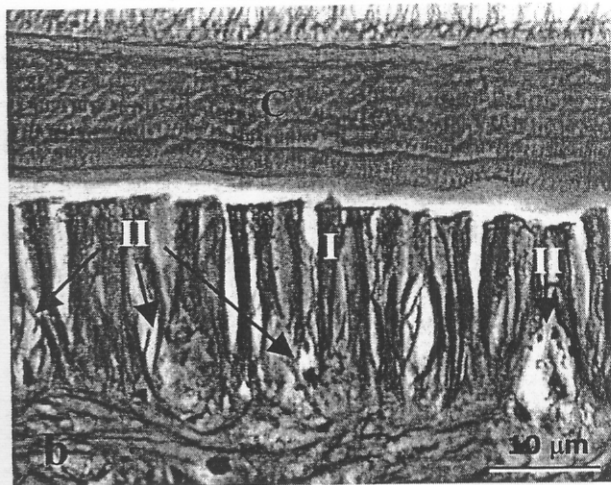
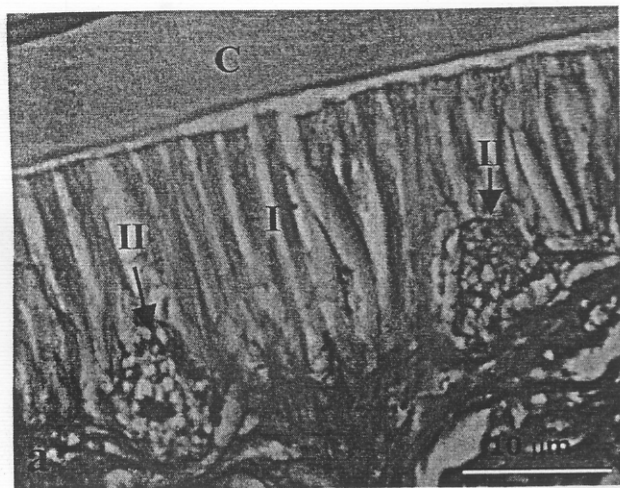


Figure 7



Figure 8

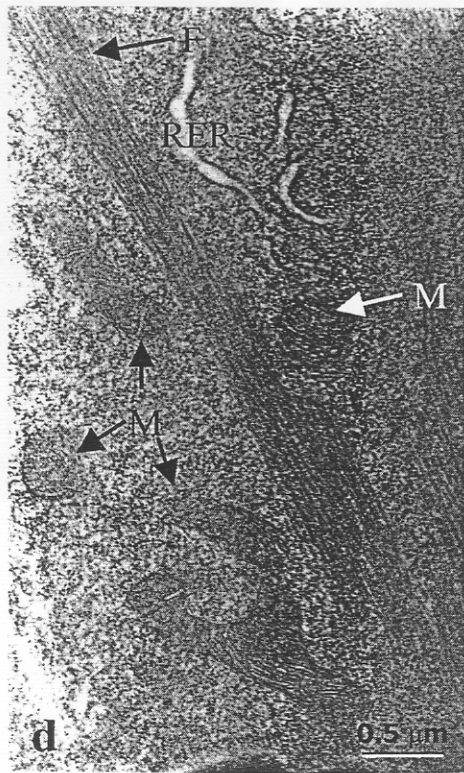
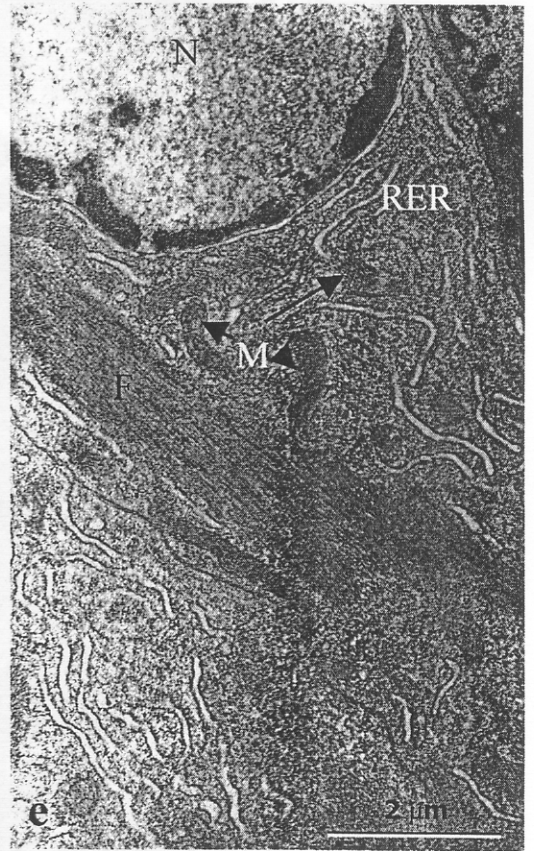
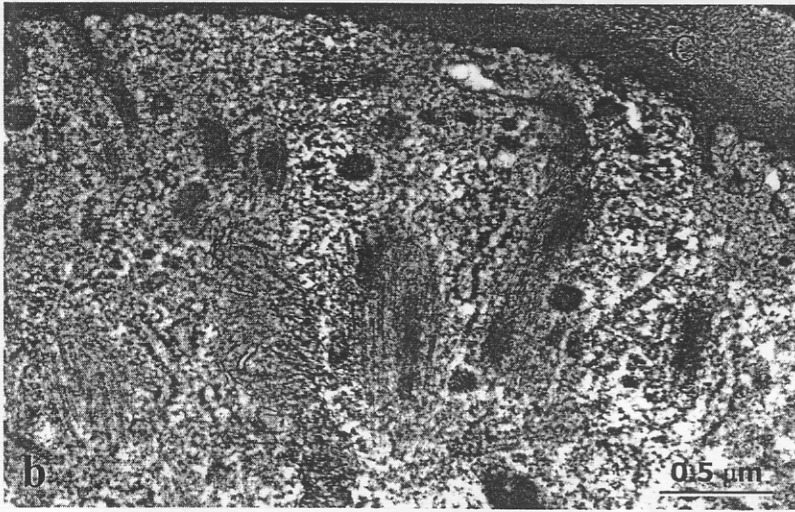
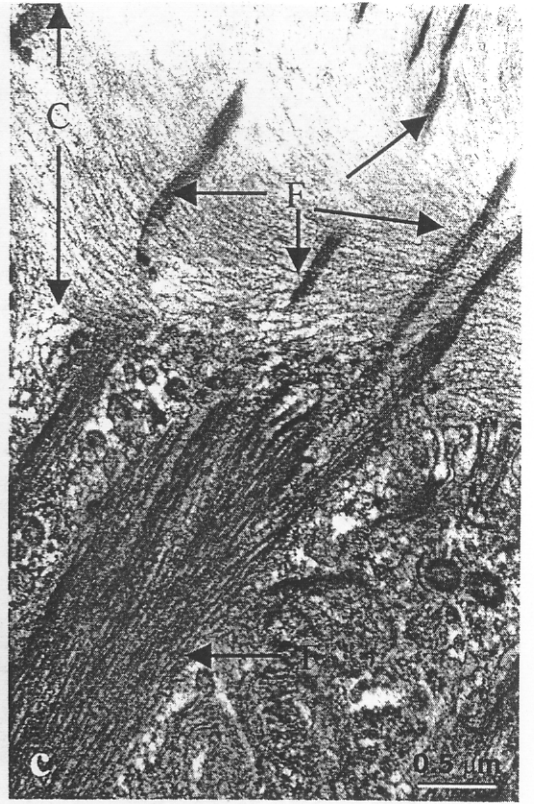
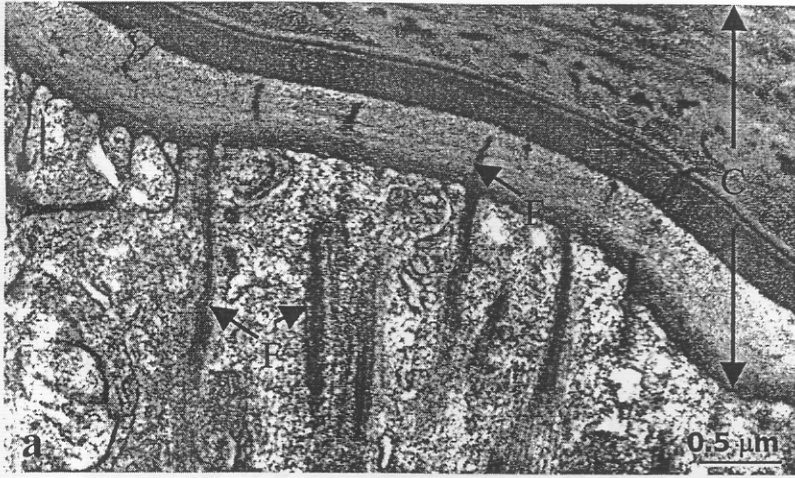


Figure 9

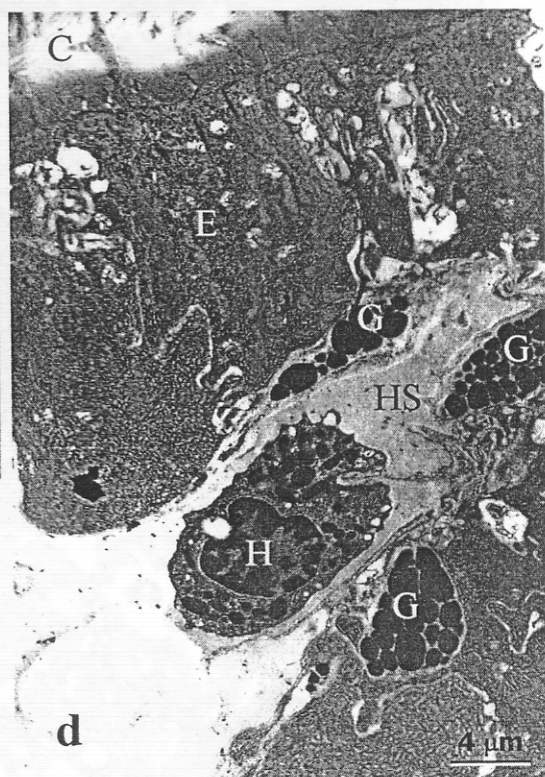
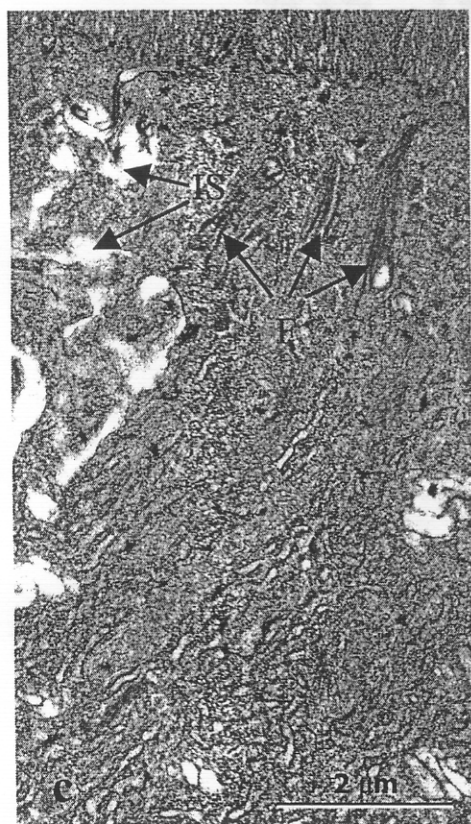
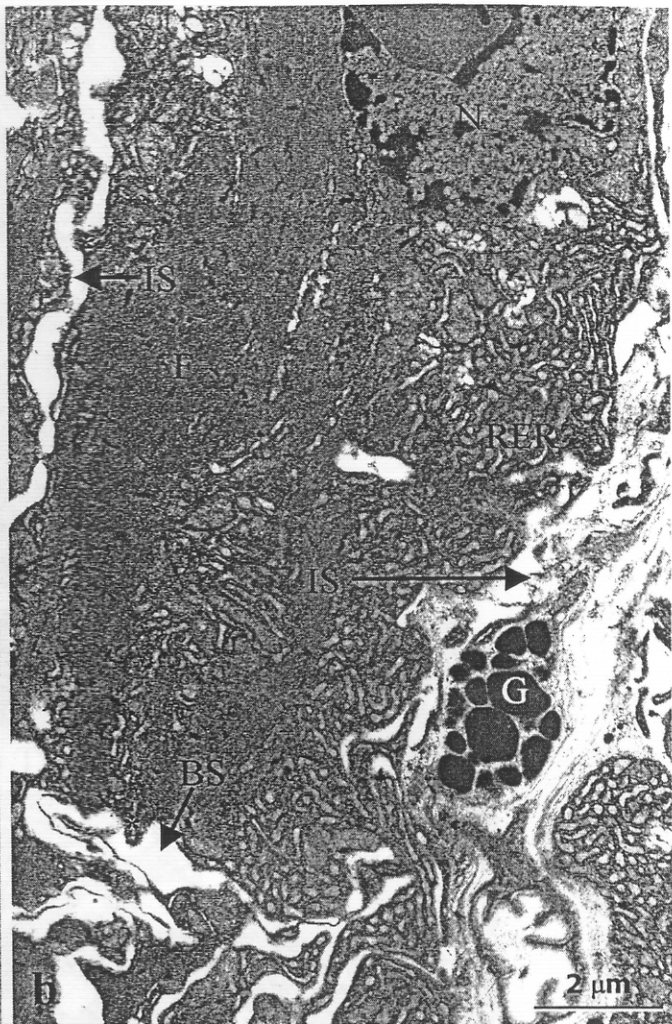
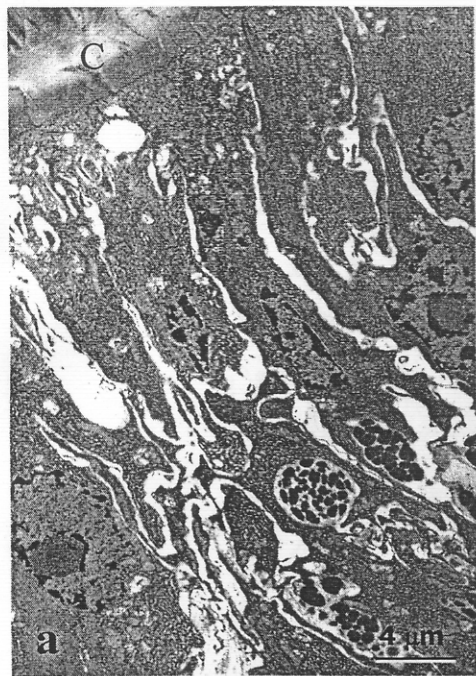


Figure 10

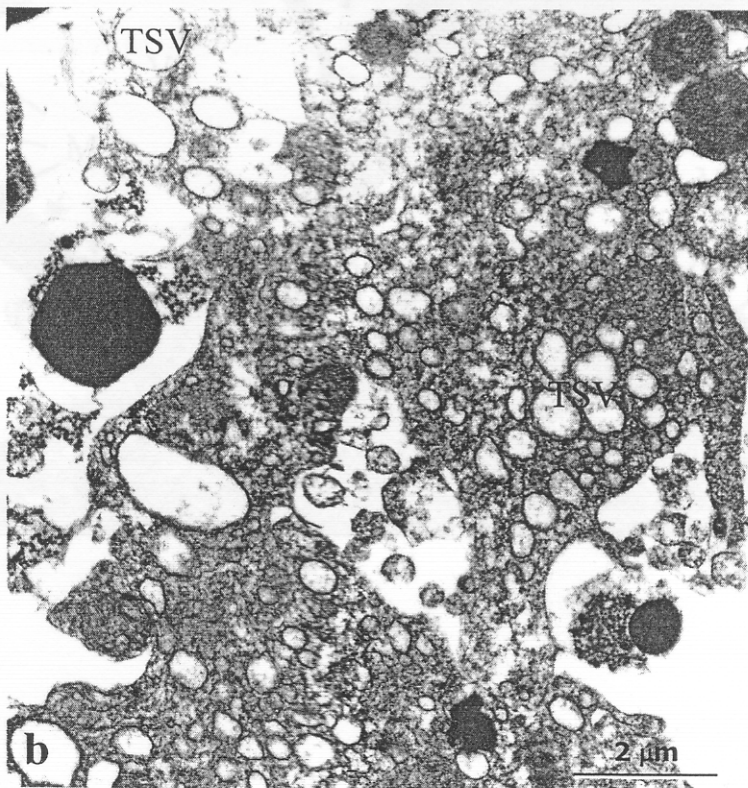
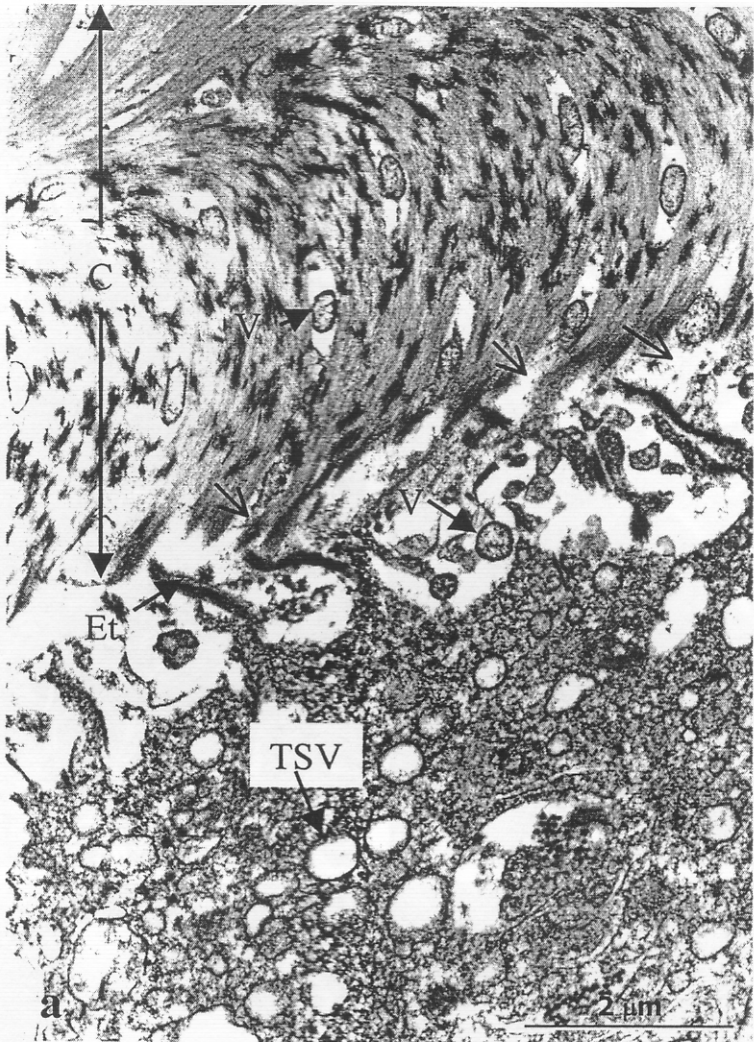


Figure 11

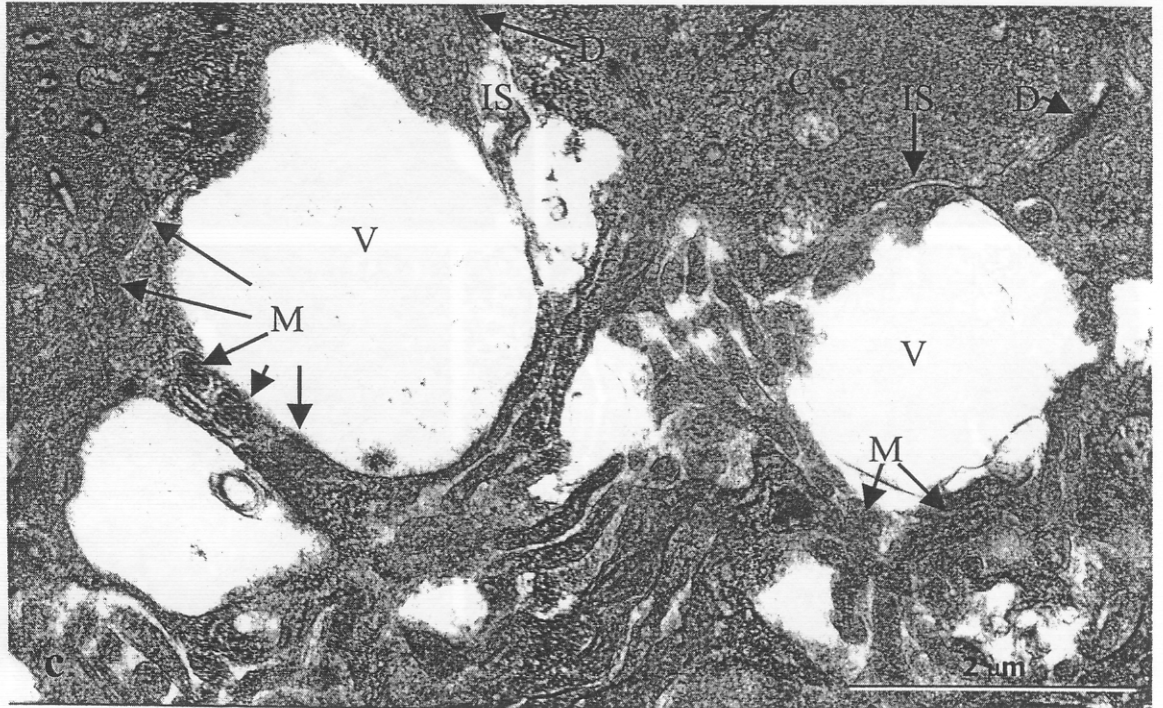
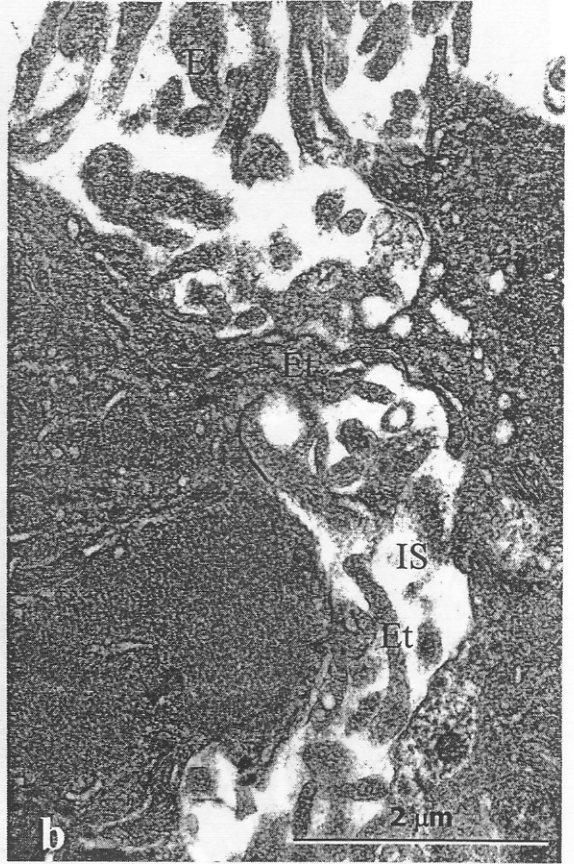
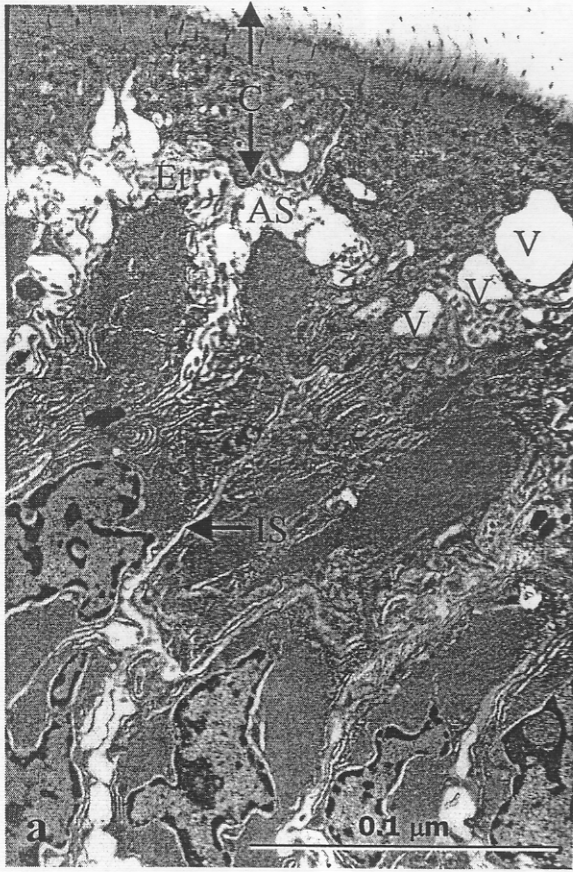


Figure 12

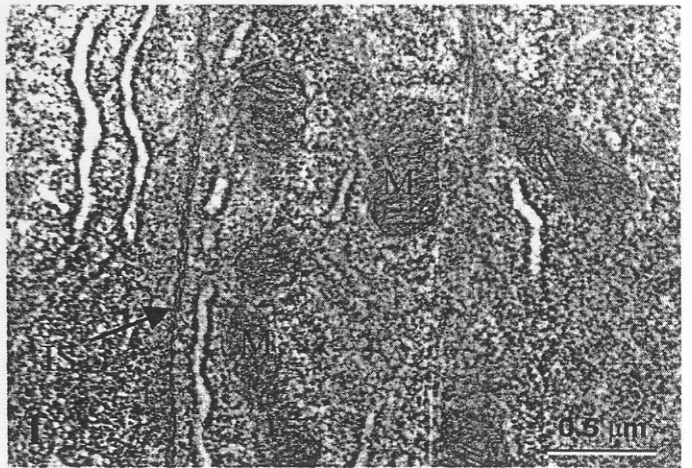
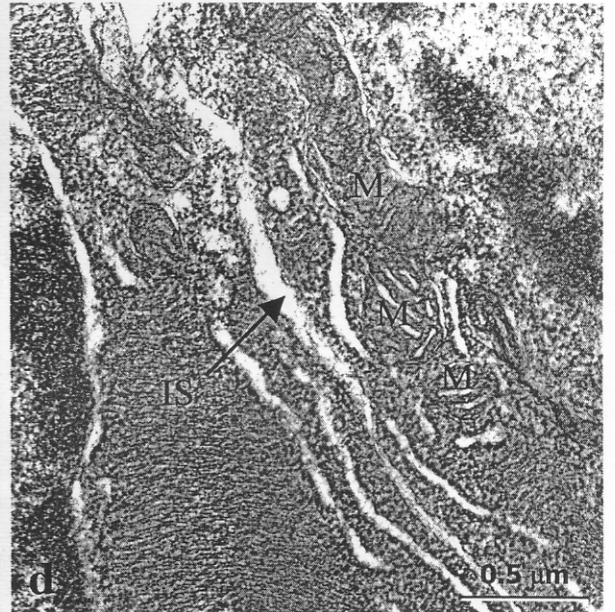
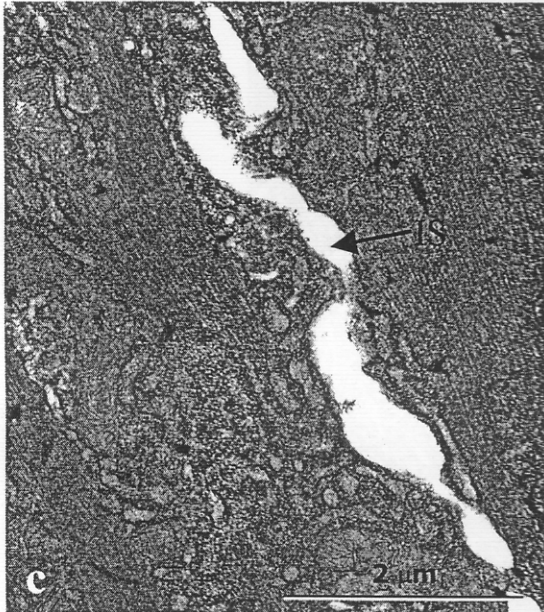
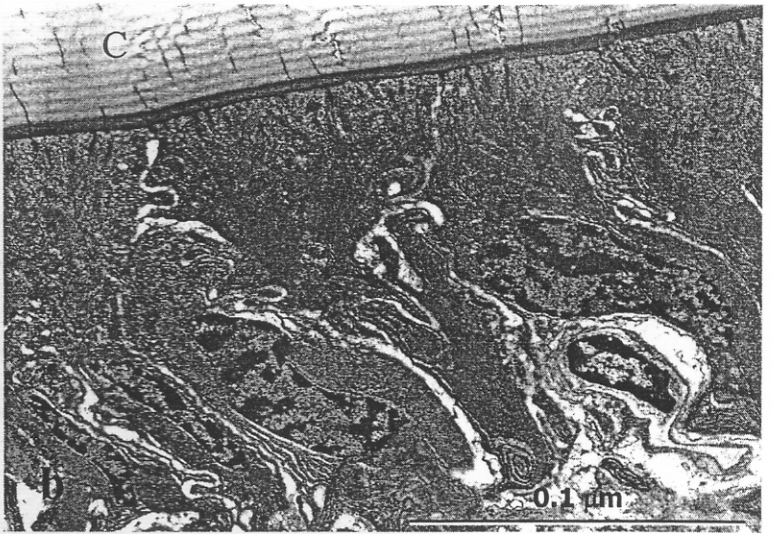
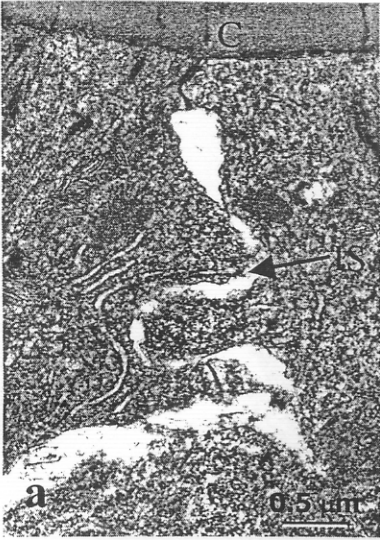


Figure 13

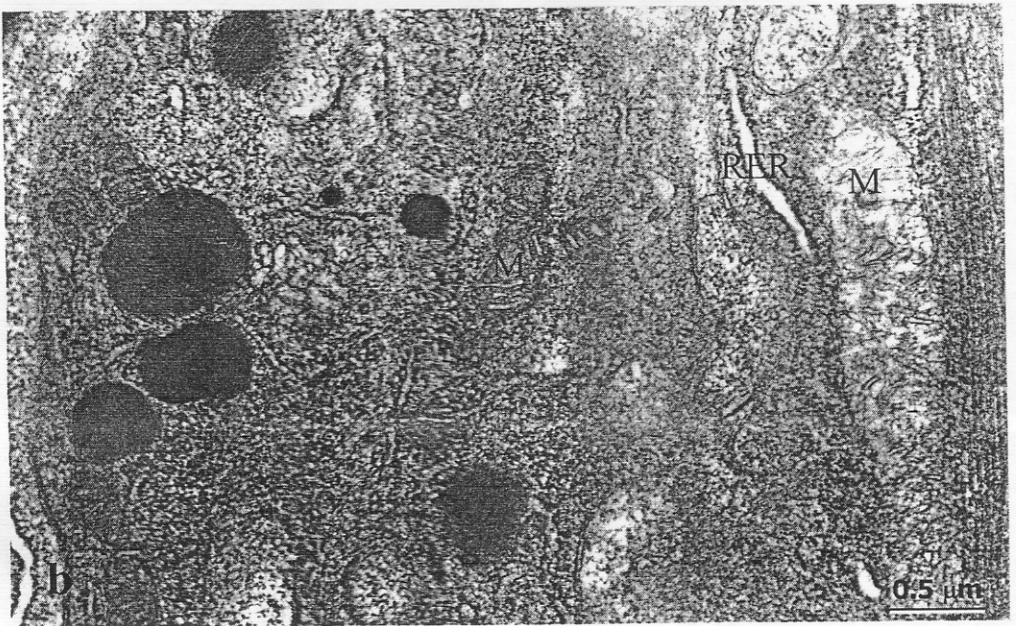


Figure 14

